CIC-14 REPORT COLLECTION

REPRODUCTION
COPY

NUREG/CR-5182
LA-11377-MS

c. 3

The Seismic Category I Structures Program: Results for FY 1986

Prepared by J.G. Bennett, R.C. Dove, W.E. Dunwoody,
C.R. Farrar, P. Goldman

Los Alamos National Laboratory

Prepared for
U.S. Nuclear Regulatory
Commission

LOS ALAMOS NATIONAL LABORATORY
3 9338 00323 3110

NOTICE

This report was prepared as an account of work sponsored by an agency of the United States Government. Neither the United States Government nor any agency thereof, or any of their employees, makes any warranty, expressed or implied, or assumes any legal liability of responsibility for any third party's use, or the results of such use, of any information, apparatus, product or process disclosed in this report, or represents that its use by such third party would not infringe privately owned rights.

NOTICE

Availability of Reference Materials Cited in NRC Publications

Most documents cited in NRC publications will be available from one of the following sources:

1. The NRC Public Document Room, 1717 H Street, N.W.
   Washington, DC 20555
2. The Superintendent of Documents, U.S. Government Printing Office, Post Office Box 37082, Washington, DC 20013-7082
3. The National Technical Information Service, Springfield, VA 22161

Although the listing that follows represents the majority of documents cited in NRC publications, it is not intended to be exhaustive.

Referenced documents available for inspection and copying for a fee from the NRC Public Document Room include NRC correspondence and internal NRC memoranda; NRC Office of Inspection and Enforcement bulletins, circulars, information notices, inspection and investigation notices; Licensee Event Reports; vendor reports and correspondence; Commission papers; and applicant and licensee documents and correspondence.

The following documents in the NUREG series are available for purchase from the GPO Sales Program: formal NRC staff and contractor reports, NRC-sponsored conference proceedings, and NRC booklets and brochures. Also available are Regulatory Guides, NRC regulations in the *Code of Federal Regulations,* and *Nuclear Regulatory Commission Issuances.*

Documents available from the National Technical Information Service include NUREG series reports and technical reports prepared by other federal agencies and reports prepared by the Atomic Energy Commission, forerunner agency to the Nuclear Regulatory Commission.

Documents available from public and special technical libraries include all open literature items, such as books, journal and periodical articles, and transactions. *Federal Register* notices, federal and state legislation, and congressional reports can usually be obtained from these libraries.

Documents such as theses, dissertations, foreign reports and translations, and non-NRC conference proceedings are available for purchase from the organization sponsoring the publication cited.

Single copies of NRC draft reports are available free, to the extent of supply, upon written request to the Division of Information Support Services, Distribution Section, U.S. Nuclear Regulatory Commission, Washington, DC 20555.

Copies of industry codes and standards used in a substantive manner in the NRC regulatory process are maintained at the NRC Library, 7920 Norfolk Avenue, Bethesda, Maryland, and are available there for reference use by the public. Codes and standards are usually copyrighted and may be purchased from the originating organization or if they are American National Standards, from the American National Standards Institute, 1430 Broadway, New York, NY 10018.

NUREG/CR-5182
LA-11377-MS
RD

The Seismic Category I Structures Program: Results for FY 1986

Manuscript Completed: June 1988
Date Published: September 1988

Prepared by
J.G. Bennett, R.C. Dove, W.E. Dunwoody
C.R. Farrar, P. Goldman

Los Alamos National Laboratory
Los Alamos, NM 87545

Prepared for
Division of Engineering
Office of Nuclear Regulatory Research
U.S. Nuclear Regulatory Commission
Washington, DC 20555
NRC FIN A7221

LOS ALAMOS NAT'L. LAB. LIBS.
3 9338 00323 3110

TABLE OF CONTENTS

ABSTRACT..... 1

I. INTRODUCTION..... 1

II. CONSTRUCTION AND TESTING: (TRG) STRUCTURES..... 8
A. Construction and Material Properties..... 8
B. Low-Level Modal and Static Tests of TRG-3 (at Los Alamos)..... 9
C. Tests Conducted at CERL..... 17

III. THEORETICAL ANALYSIS OF THE TRG STRUCTURE..... 21
A. Design Method..... 21
B. Structural Dynamics Method..... 23
C. Finite Element Method..... 23

IV. COMPARISON OF EXPERIMENTAL RESULTS FROM TRG-1 AND TRG-3..... 24

V. COMPARISON OF THEORETICAL AND EXPERIMENTAL RESULTS..... 36

VI. CONCLUSIONS..... 42

VII. REFERENCES..... 43

APPENDICES

A. SAMPLE OF CALCULATIONS INVOLVED IN THE DESIGN METHOD..... 44
B. A STRUCTURAL DYNAMICS METHOD OF ANALYZING TRG-3..... 49

LIST OF FIGURES

1. Isolated shear wall structure..... 3
2. Two-story diesel generator building, models and prototype..... 4
3. Idealized three-story auxiliary building, models and prototype..... 5
4. TRG-3 model..... 7
5. TRG-3 under construction..... 11
6. Schematic presentation by modal analysis software of TRG 1-in.-wall model showing 31 points at which data are collected. Point 2 is the load application point..... 12
7. Modal testing the TRG structure at Los Alamos..... 13
8. Static load frame details..... 15
9. Locations of the linear voltage differential transformer displacement measurements taken during the static testing of the TRG-3 structure..... 16
10. Modal testing in the free-free mode at CERL with the structure suspended from nylon straps..... 18
11. Method used to attach TRG-3 to CERL shaker..... 19

LIST OF FIGURES

12. Schematic showing the locations of the accelerometer on the TRG-3 structure 20
13. Haversine pulse used in the TRG-3 test 21
14. One-quarter model finite element mesh used for finite element calculations 24
15. Computational model used to study the base connection effects 31
16. Command signal, base and top accelerometer records from haversine pulse applied to TRG-3 at CERL 32
17. Real and imaginary parts of the transfer function for the top slab accelerometer to the base for the time histories of Fig. 16 33
18. Transfer function computed from the time history of node 4 to node 2 for the computational model of Fig. 15 34
19. Time history of node 2 for the computer model of Fig. 15 34
20. Time history of node 4 for computer model of Fig. 15. $K_S/K_T \approx 0.1$ 35
21. "Command" signal applied to node 1 model of Fig. 15 35
22. Transfer function of node 4 to node 2 for model of Fig. 15 with $K_{STRUCTURAL} = K_{THEORY}$ and base connection springs lowered to give 7.7 Hz 37
23. Transfer function of node 4 to node 1 for model of Fig. 15. $K_{ST}/K_T \approx 1$, base connection lowered to give 7.7 Hz 37
24. Time history of node 2 with base connection lowered to give 7.7 Hz and $K_{STRUCTURAL}$ set to theory 38
25. Time history of node 4 with base connection springs adjusted to give 7.7 Hz and $K_{STRUCTURAL}$ set to theory 38

A-1 Cross section of TRG-3 showing the definition of the distances needed for the transformed section property calculations 45

B-1 Definitions of the coordinates used in this analysis 50

B-2 The combination of shapes used to define the shape function in the analysis 51

LIST OF TABLES

I. Computed Characteristics of the TRG Structure 8
II. Material Properties 10
III. Characteristics of the TRG Structures 12
IV. TRG Test Sequence 22
V. Comparison of Three Methods of Analysis 25
VI. Measured and Predicted Modal Frequencies and Stiffnesses 26
VII. Effective Masses and Theoretical Stiffnesses 39
VIII. Comparison of Experimentally and Theoretically Determined Values of Stiffness 40

B-1. Constants Used and Results 55

THE SEISMIC CATEGORY I STRUCTURES PROGRAM: RESULTS FOR FY 1986

by

Joel G. Bennett, Richard C. Dove, Wade E. Dunwoody,
Charles R. Farrar, and Peggy Goldman

ABSTRACT

The accomplishments of the Seismic Category I Structures Program for FY 1986 are reported. The background leading to the FY 1986 Program Plan is summarized and the design of a new geometric configuration of a reinforced concrete shear wall test structure is described. The report discusses static and seismic testings of two of these structures, a 1/4-scale, 1-in.-thick shear wall model of microconcrete and a 4-in.-thick shear wall prototype. Results and conclusions regarding degrading stiffness characteristics, natural frequencies, and scalability of microconcrete with actual concrete are compared with past fiscal year results. Possible base rotation effects for the large structure are examined analytically. Finally, tentative conclusions are stated regarding the degrading stiffness and scaling of these structures and recommendations are made about future seismic testing of large structures.

I. INTRODUCTION

The Seismic Category I Structures Program is being carried out at the Los Alamos National Laboratory under sponsorship of the U.S. Nuclear Regulatory Commission (NRC), Office of Nuclear Regulatory Research, and has the objective of investigating the structural dynamic response of Seismic Category I reinforced concrete structures (exclusive of containment) that are subjected to seismic loads beyond their design basis. The program, as originally conceived,

is a combined experimental/analytical investigation with heavy emphasis on the experiment component to establish a good data base. A number of meetings and interactions with the NRC staff have led to the following set of specific program objectives:

1. to address the seismic response of reinforced concrete Category I structures other than containments;
2. to develop experimental data for determining the sensitivity of structural behavior in the elastic and inelastic response range of Category I structures to variations in configuration, design practices and earthquake loading;
3. to develop experimental data to enable validation of computer programs used to predict the behavior of Category I structures during earthquake motions that cause elastic and inelastic response;
4. to identify floor response spectra changes that occur during earthquake motions that cause elastic and inelastic structural response; and
5. to develop a method for representing damping in the inelastic range, and demonstrate how this damping changes when structural response goes from the elastic to the inelastic ranges.

The prevailing feature of the typical structure under investigation is that shear rather than flexure is dominant; that is, the ratio of displacement values, calculated from terms identified with shear deformation, to the values contributed from bending deformation is one or greater. Thus, these buildings are called "shear wall" structures. The background of the program and its status leading to the work reported here will be briefly summarized below.

The Seismic Category I Structures Program began in FY 1980 with an investigation that identified the typical nuclear shear wall structure and its characteristics (stiffnesses, frequencies, etc.) as being the most important and least understood seismic resisting structure. A combined experimental/analytical plan for investigation of the dynamic behavior of these structures was laid out as described in Ref. 1. During the first phase, the program concentrated on investigating isolated shear wall behavior using small models (1/30-scale, 1-in. wall thickness, Fig. 1) that could be economically constructed and tested both statically and dynamically. The results of these investigations are reported in Ref. 2. During this early phase of the program, a Technical Review Group (TRG) consisting of nationally recognized

seismic and concrete experts on nuclear civil structures was established to both review the progress and make recommendations regarding the technical direction of the program. The recommendations of this group have been evaluated in light of the needs of the USNRC and, when possible, have been carefully integrated into the program.

Following the isolated shear wall phase, the program began testing and evaluating 3-D box-like structures, which represented idealized diesel generator buildings (Fig. 2). It was recognized from the outset that scale model testing of concrete structures is a controversial issue in the U.S. civil engineering community. Thus, two sizes of structures were tested in an effort to demonstrate scalability of results. This work is reported in Refs. 3-5. Other variables of interest, especially the effect of number of stories, were investigated by constructing, analyzing, and testing small-scale structures representative of a typical three-story auxiliary building. The results obtained from the tests of these structures, shown in Fig. 3, are given in Ref. 6.

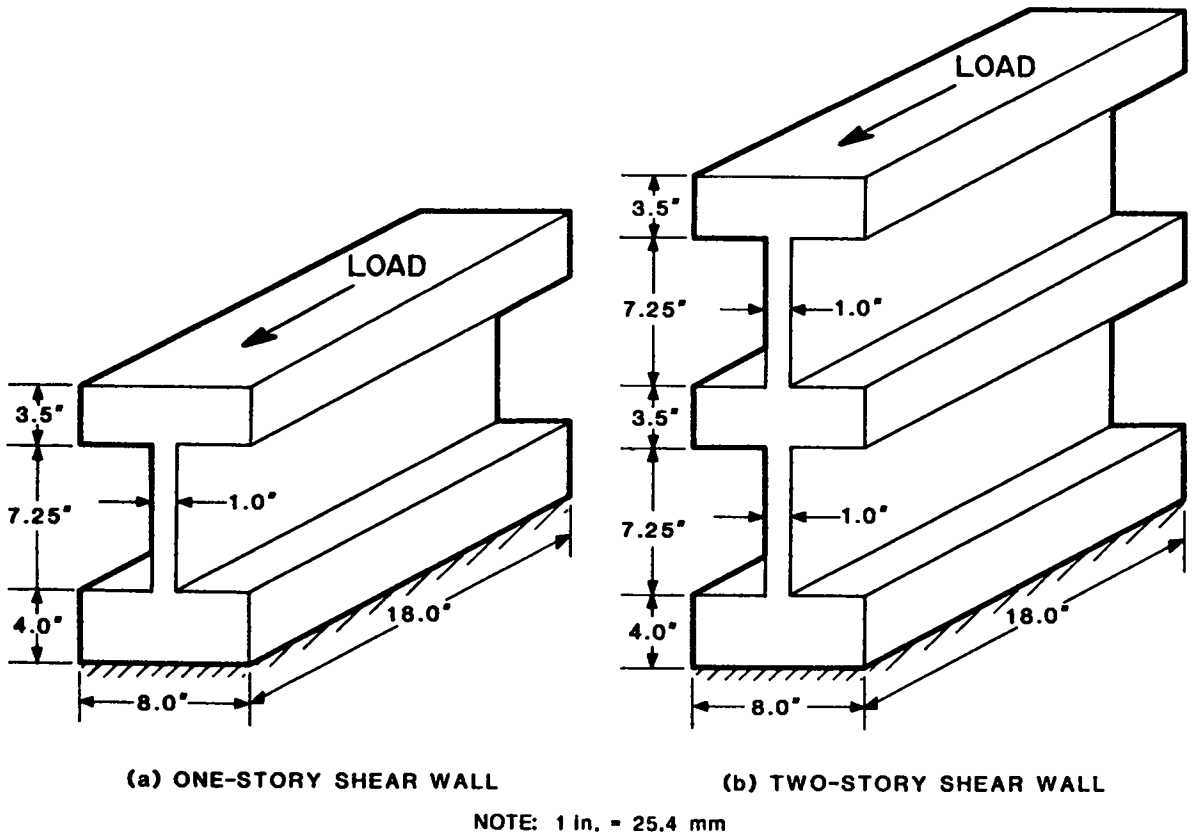

Fig. 1. Isolated shear wall structure.

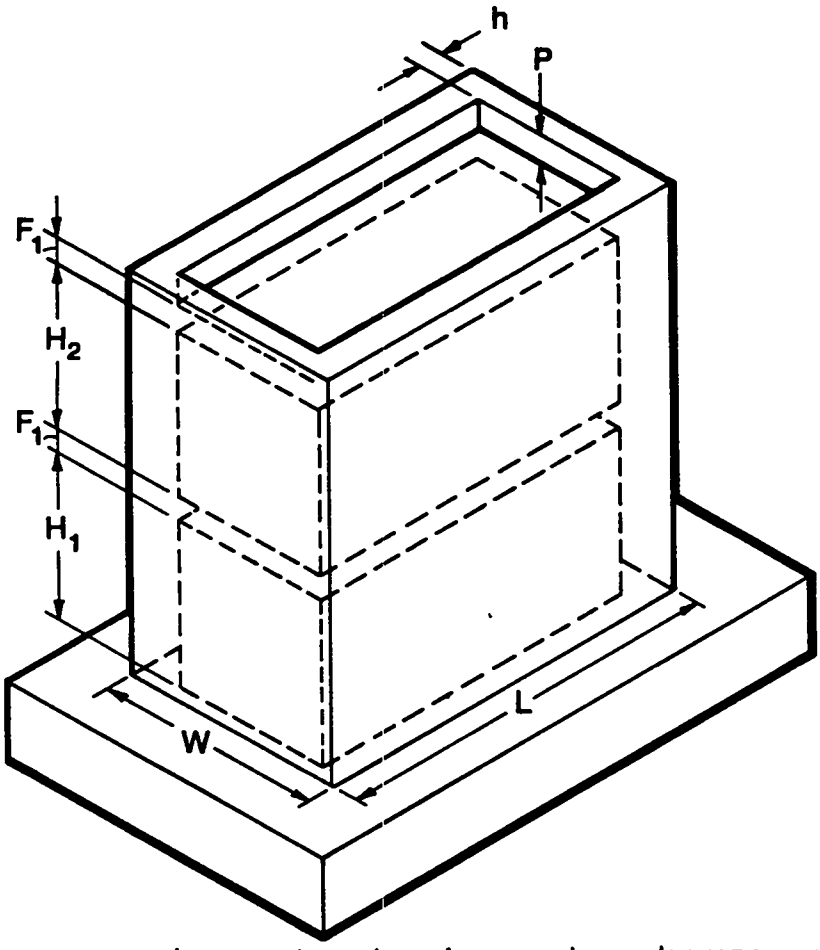

	h, F_1, F_2	W	L	H_1 & H_2	P	Wt/STORY *
1/30-SCALE	1 in.	10 in.	18 in.	7.25 in.	1 in.	47.7 lb
1/10-SCALE	3 in.	30 in.	54 in.	21.75 in.	3 in.	1286 lb
PROTOTYPE	30 in.	25 ft	45 ft	18.125 ft	30 in.	1,286,000 lb

*BASE NOT INCLUDED

NOTE: 1 in. = 25.4 mm, 1 ft = 0.305 m, 1 lb = 4.45 N

Fig. 2. Two-story diesel generator building, models and prototype.

Although a number of results on items such as aging (cure time), effect of increasing seismic magnitude, etc., had been reported, the two most important and consistent conclusions coming out of the data from this program are: first, the scalability of the results between microconcrete models of different sizes was illustrated both in the elastic and inelastic range; second, the so-called "working load" secant stiffness of the models was lower than the computed uncracked cross-sectional values by a factor of about 4. The term

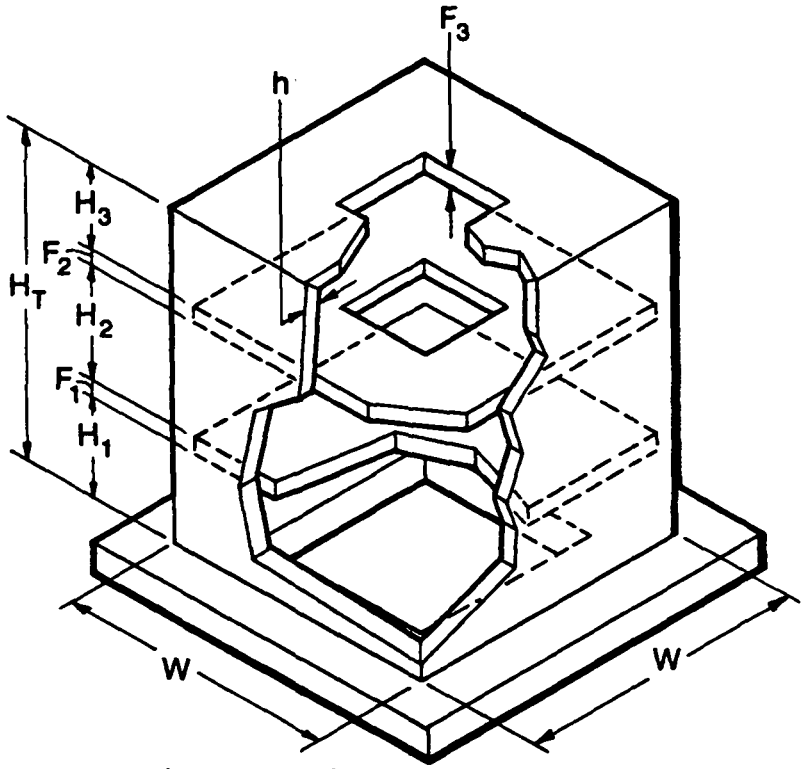

	h, F_1, F_2, F_3	W	H_1, H_2, H_3	Wt/STORY*
1/42-SCALE	1 in.	26 in.	10 in.	140 lb
1/14-SCALE	3 in.	78 in.	30 in.	3780 lb
PROTOTYPE	42 in.	1092 in.	420 in.	10,372,000 lb

* BASE NOT INCLUDED

NOTE: 1 in. = 25.4 mm, 1 lb = 4.45 N

Fig. 3. Idealized three-story auxiliary building, models and prototype.

"working load" is meant in the sense of loads that produce stress levels equivalent to at least the design basis earthquake and up to the safe shutdown earthquake.

During their review of this program, the TRG pointed out the following:

1. Design of prototype nuclear plant structures is normally based on an uncracked cross section strength-of-materials approach which may or may not use a "stiffness reduction factor" for the concrete, but if one is used it is never as large as 4.

2. Although the structures themselves appear to have adequate reserve margin (even if the stiffness is only 25% of the theoretical value), any piping and attached equipment will have been designed using inappropriate floor response spectra.

3. Given that a nuclear plant structure designed to have a natural response of about 15 Hz may have a natural frequency of 7.5 Hz (corresponding to a reduction in stiffness of 4), and allowing further that the natural frequency may further decrease because of degrading stiffness, the natural response of the structure will shift well down into the frequency range for which an earthquake's energy content is the largest. This shift will result in increased amplification in the floor response spectra at lower frequencies, and this fact has a potential impact on the equipment and piping design response spectra and their margins of safety.

Note that all three points are related to the difference between measured and calculated stiffnesses of these structures.

Having made these observations, several questions arise. Do the previous experimental data taken on microconcrete models represent data that would be observed on prototype structures? What is the appropriate value of the stiffness that should be used in design and for component response spectra computations in these structures? Should it be a function of load level? Have the equipment and piping in existing buildings been designed to inappropriate response spectra? What steps should be taken to evaluate this reduced stiffness for existing structures?

Thus, starting in FY 1985, the primary program emphasis was to ensure credibility of previous experimental work by beginning to resolve the difference between the analytical and theoretical stiffness that came to be called the "stiffness difference" issue. The TRG for this program believed that this important issue should be addressed before other program objectives could be accomplished.

For these stiffness-related concerns, it was agreed that a series of credibility experiments would be carried out using both large- and small-scale structures. For the large-scale structure, the TRG set limitations on the design parameters. Their recommended "ideal" structure characteristics, in order of decreasing priority, were as follows:

1. Maximum predicted bending and shear mode natural frequency $\leq$30 Hz.
2. Minimum wall thickness = 4 in.
3. Height-to-depth ratio of shear wall $\leq$ 1.
4. Use actual No. 3 rebar for reinforcing.
5. Use realistic material for aggregate.
6. Use 0.1% to 1% steel (0.3% each face, each direction ideally).

7. Use water-blasted construction joints to ensure good aggregate frictional interlock.

A structure, called the TRG structure and shown in Fig. 4, was specifically designed to meet these requirements. The computed characteristics of this structure are given in Table I. However, it was decided that, before constructing this relatively large and expensive (both to build and especially to test) structure, a smaller (1/4)-scale model of the proposed structure should be designed, constructed, and tested.

The purposes of this 1/4-scale microconcrete model were as follows: first, by applying the same principles of analysis and design, and the same construction practices as were used in the previous work, the scalability of the results of a microconcrete model to a prototype structure of "real" concrete could be investigated. Second, conclusions (based on calculations) concerning the model and prototype torsional response, individual wall frequencies, out-of-plane bending, and other features that affect the response of the large TRG

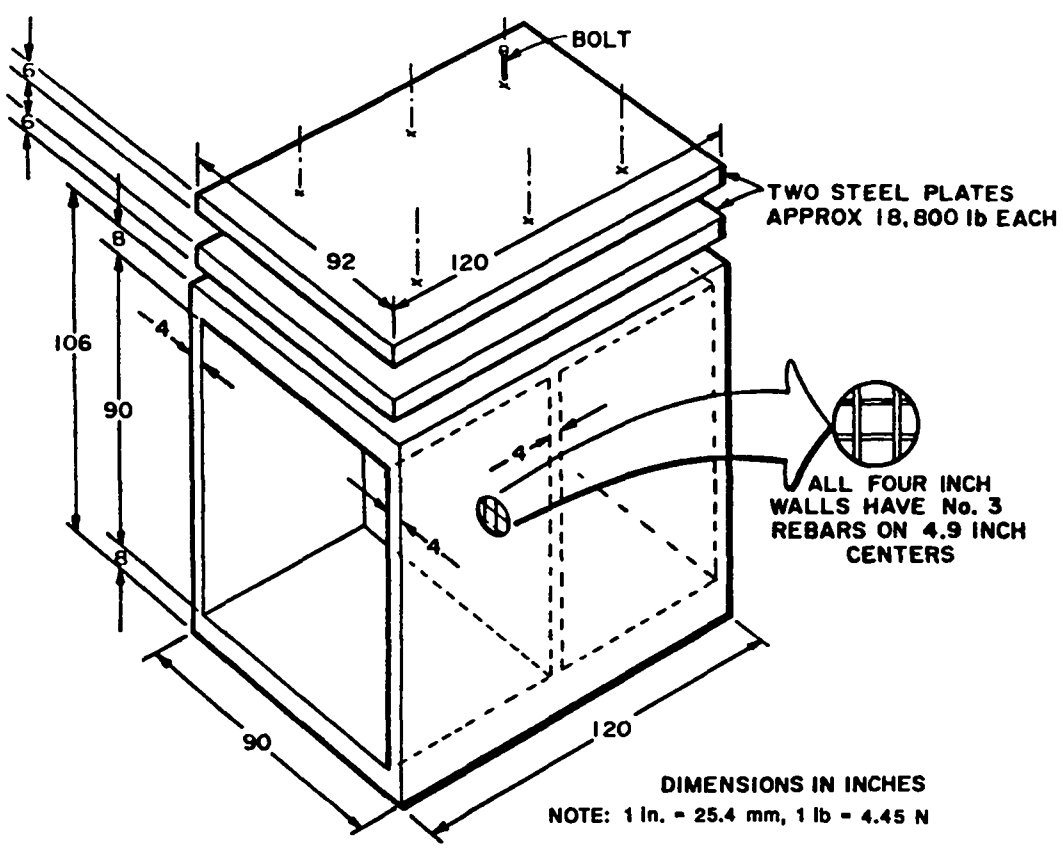

Fig. 4. TRG-3 model.

TABLE I

COMPUTED CHARACTERISTICS OF THE TRG STRUCTURE

Wall thickness	= 4 in.
$I_{uncracked}$ transformed section including steel	= 2.06×10^6 in.^{4}
A-effective shear area	= 379 in.^{2}
Area total (plan view)	= 1288 in.^{2}
Total uncracked bending stiffness	= 2.5×10^7 lb/in.
Shear stiffness	= 5.3×10^6 lb/in.
Total stiffness	= 4.2×10^6 lb/in.
Max dead weight normal stress	= 42 psi
Max shear stress in flange at 5g due to assumed 5% torsion (approx.)	= 35 psi
Total concrete	= 6 yd.^{3}
Total added weight	= 37,000 lb
Total weight	= 61,000 lb

structure can be confirmed on a less expensive test structure. Third, instrumentation and other data acquisition requirements could be worked out before the larger-scale tests. The construction, analysis, testing, and results from the investigation of the 1/4-scale microconcrete model of the TRG structure are discussed in Ref. 7.

This report covers the construction, analysis, testing, and results from the full-size TRG structure (Fig. 4). In addition, because it is desirable to compare the results from the tests on the 1/4-scale model to the results from the tests on the full-size structure, this report contains results from the 1/4-scale model tests, some of which were previously reported (Ref. 7).

II. CONSTRUCTION AND TESTING: (TRG) STRUCTURES

As mentioned in the preceding introduction (and detailed in Ref. 7), during FY 1985 the TRG for this project recommended the construction, analysis, and testing of a "real" concrete structure designed to meet specific criteria. The TRG structure, shown in Fig. 4 and having the characteristics given in Table I, was constructed, analyzed, and tested during FY 1986.

A. Construction and Material Properties

Because several TRG structures were planned, the following identification system has been adopted:

TRG — Designed to fulfill the objectives proposed in consultation with the project Technical Review Group

Model No.	Order of construction
WT	Shear wall element thickness-inches
AR	Shear wall aspect ratio (height to length)
%R	% reinforcement.

Thus, TRG-No.-WT (AR, %R) is used as the notation.
For the 1/4-scale, microconcrete model,

TRG-1-1 (1, 0.56), abbreviated as TRG-1; and

for the first full-size structure,

TRG-3-4 (1, 0.60*), abbreviated as TRG-3.

The material properties of TRG-3 are given and compared to TRG-1 material properties in Table II.

Both TRG structures (TRG-1 and TRG-3) were constructed at Los Alamos by Los Alamos personnel. The larger structure (TRG-3) was constructed on the test stand which was later used as the modal vibration and static loading test base so as to minimize handling before preliminary tests could be completed. Figure 5 shows the larger structure (TRG-3) under construction.

The resulting "as built" characteristics of the two structures are given and compared with the design values in Table III.

B. Low-Level Modal and Static Tests of TRG-3 (at Los Alamos)

The low-load-level testing for the structure began during the week of December 16, 1985. The structure was placed on foam pads for modal testing as a "free-free" structure to characterize the very low-level vibrational frequencies and thus the structural "as-built" stiffnesses. First, a series of hammer tap tests was used to excite the structure. Second, a 300-lb-force portable shaker was used to excite the structure with a random signal having a frequency content of 0-500 Hz. For both modal analysis tests, accelerometer data were taken at 31 points, shown schematically in Fig. 6 in three orthogonal directions. Figure 7 illustrates this operation. These tests gave some natural frequency and mode shape information, but the foam pads did not allow a true "free-free" condition to be simulated and coherence for the test signals below 200 Hz was poor.

---

* A second, 1/4-scale structure [TRG-2-1 (1, 0.56)] was constructed but was not completely tested because of obvious flaws and is not reported on.

TABLE II

MATERIAL PROPERTIES

Concrete	TRG-3	TRG-1
E_c, psi	= (measured at σ-ε origin = 2.0×10^6	3.18×10^6
f'_c, psi	= (compressive strength) = 3807	3769
f_t, psi	= (split tensile test strength = 351	513
E'_c, psi	= $57000\sqrt{f'_c} = 3.52 \times 10^6$	3.49×10^6
Steel		
E, psi	= 30×10^6	25.6×10^6
Yield, Strength, Ksi	= 40 min.	42.7
Ultimate Strength, Ksi	= 70 min.	53.1
Elongation at failure, %	= 11 min.	4%
Diameter, in.	= 3/8	0.042
Steel reinforcing 0.6% both directions (No. 3 rebar)		0.56% both directions (0.042in. diam. galv. hardware screen)
Note: The values for steel are "handbook" values <u>not</u> measured.		Note: These values for steel are measured values

Next, the base of the structure was bolted to its support plate and a load frame, specifically constructed for low-load-level (less than 80 psi maximum principal stress) static testing, was assembled (Fig. 8). These tests were completed during the week of December 23, 1985. The 37,600 lb of added weights arrived after the tests had been completed and were fitted to the structure during the week of December 27, 1985, and the transfer functions of the top slab acceleration to the base slab acceleration records were measured. The structure was shipped to the Construction Engineering Research Laboratory (CERL) at Champaign, Illinois, on January 2, 1986.

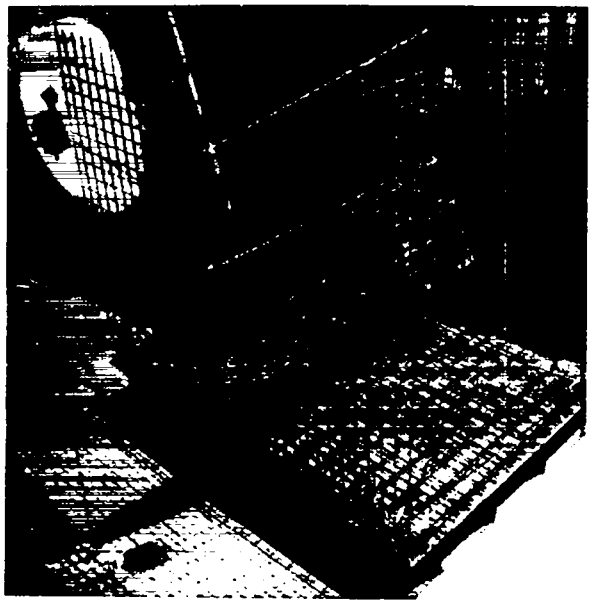

(a)

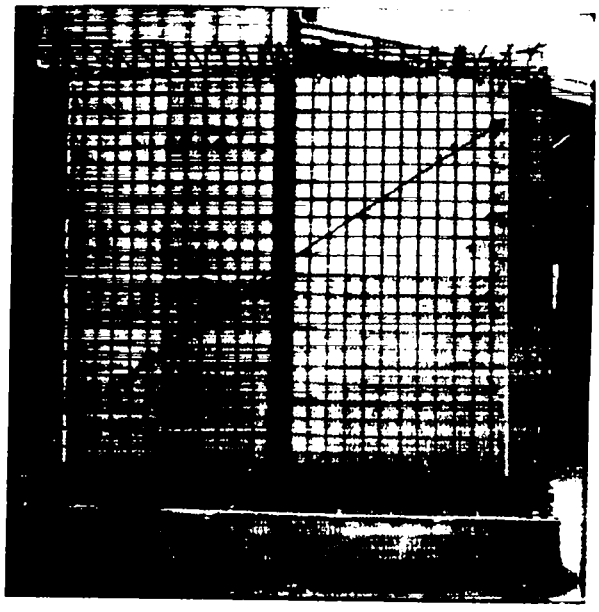

(b)

(c)

Fig. 5. TRG-3 under construction.

TABLE III

CHARACTERISTICS OF THE TRG STRUCTURES

Property	TRG-3 Design Value*	TRG-3 As-Built Value**	TRG-1 Design Value*	TRG-1 As-Built Value**
Uncracked section moment of inertia (I_t), in.^{4}	2.06×10^6	2.15×10^6	8.05×10^3	8.39×10^3
Area effective shear (transformed), in.^{2}	379	376	23.7	23.5
Area (total), in.^{2}	1288	1288	80.5	80.5
Total uncracked cantilever bending stiffness ($3E_cI_t/L^3$), lb/in.	2.5×10^7	3.10×10^7	0.625×10^7	0.78×10^7
Shear stiffness (A_eG/L), lb/in.	5.3×10^6	6.1×10^6	1.33×10^6	1.53×10^6
Mass contribution ($2E_cI_t/hL^2$), lb/in.	2.5×10^8	3.15×10^8	0.625×10^8	0.79×10^8
Total stiffness, lb/in.	4.3×10^6	5.09×10^6	1.08×10^6	1.27×10^6
Max. dead weight normal stress psi	42	----	10.5	----
Max. shear stress in flange due to assumed 5% torsion (approx), psi	35 (at 5 g)	----	35 (at 20 g)	----
Total concrete, cubic yards	6	----	0.1	----
Total added weight, lb	37,000	37,600	578	575
Total Weight, lb	61,000	61,600	953	950

* Calculated using $E_c = 3.0 \times 10^6$ lb/in.^{2} as the design value.
**Calculated using $E_c = 3.5 \times 10^6$ lb/in.^{2} from $57{,}000\sqrt{f'_c}$.

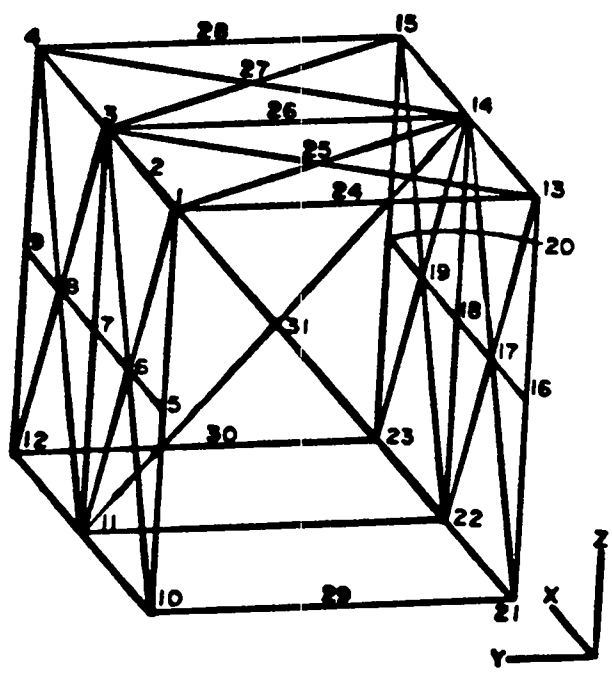

Fig. 6. Schematic presentation by modal analysis software of TRG 1-in.-wall model showing 31 points at which data are collected. Point 2 is the load application point.

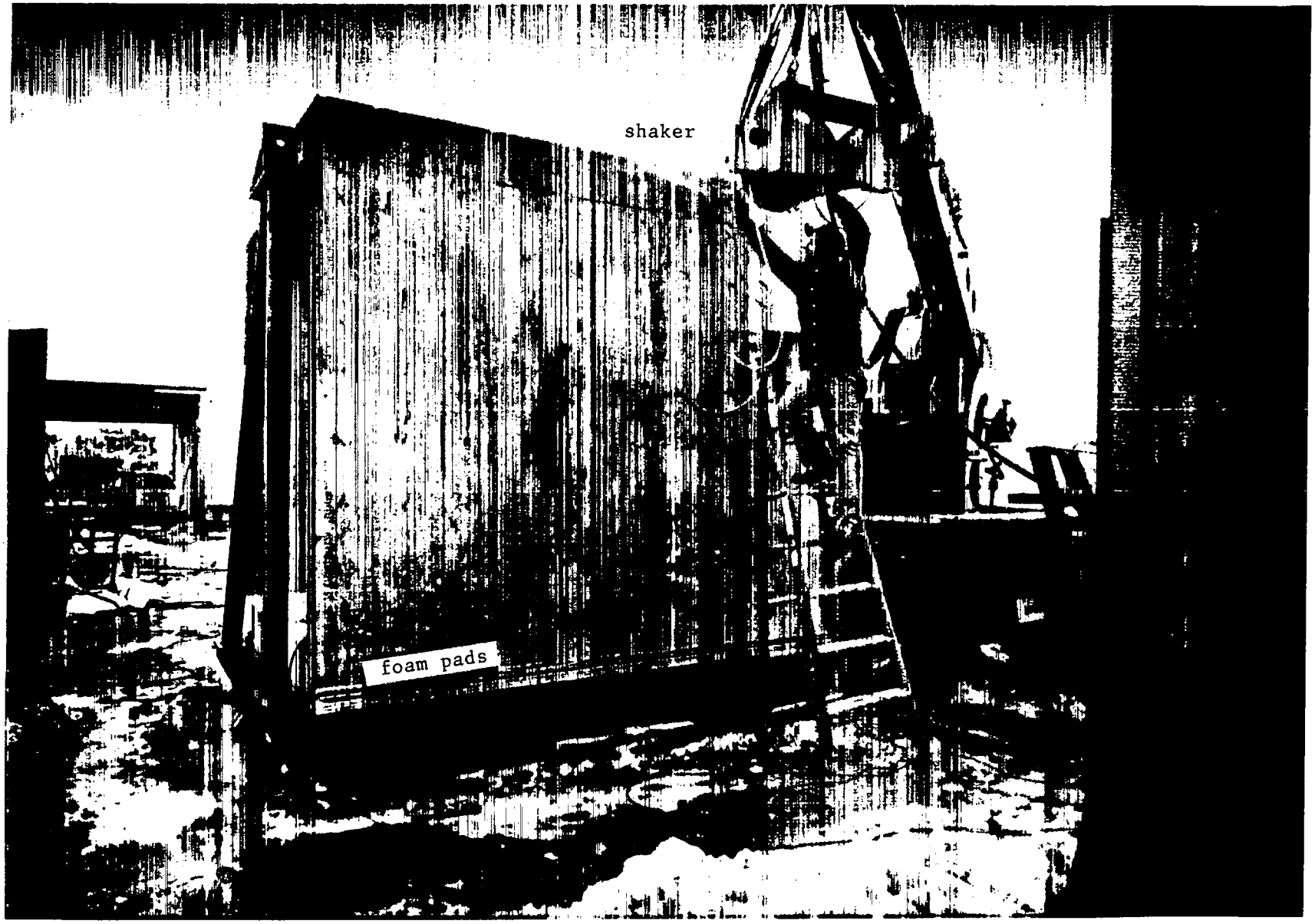

Fig. 7. Modal testing the TRG structure at Los Alamos.

This low-load-level testing (monotonic static and modal), which was conducted before the structure was shipped to CERL for simulated seismic testing, was undertaken to serve several purposes. First, the initial as-built stiffness of the structure was desired for comparison with theory, second, for comparison with similar test results that would be taken after shipping, and third, for comparison with similar test results from the 1/4-scale model of this structure (TRG-1). The third comparison was meant to investigate scalability between "micro" and "real" concrete at low-load levels.

These initial modal tests were failures in the sense that the analysis of the data failed to accurately indicate modal frequencies associated with a clearly defined test condition (i.e., free-free vibration). For the modal tests at CERL, the structure was suspended from an overhead crane, thus better simulating free-free conditions.

The displacement measurements made during the statics test series are described in Fig. 9. The figure shows that fifteen linear variable differential transformers (LVDT) were used during the test. A maximum load of 10,000 lb was incrementally applied during the tests, corresponding to an average base shear stress of 28 psi at the 10,000-lb load level. The load was applied in one direction only, and the test was repeated four times. Data from LVDTs and the load cell were recorded using a Hewlett-Packard 9825 data acquisition system.

Studies of the data demonstrated two problems. Motion of the model relative to the frame supporting the external LVDTs introduced some distortion into the readings. In addition, the magnitudes of the displacements encountered at several of the key LVDT locations were less than the resolution range of the LVDTs. These characteristics of the measuring system reduced the validity of the results that could be obtained from the external LVDTs (Nos. 9-15, Fig. 9). However, the data from the internal LVDTs (7 and 8) were adequate to obtain a good value for the low-load-level stiffness of the model. This calculation is based upon work reported in Ref. 8.

The average shear strain within the area of the model covered by the diagonal displacement gages was shown to be

$$\gamma_{avg} = \frac{|\Delta 7| + |\Delta 8|}{L_i},$$

where $\Delta 7$ = change in length of one diagonal,

$\Delta 8$ = change in length of the other diagonal, and

L_i = initial length of the diagonal.

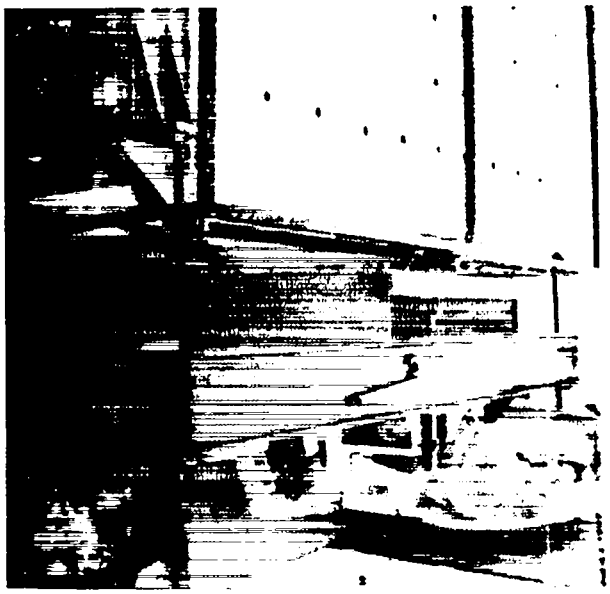

(a)

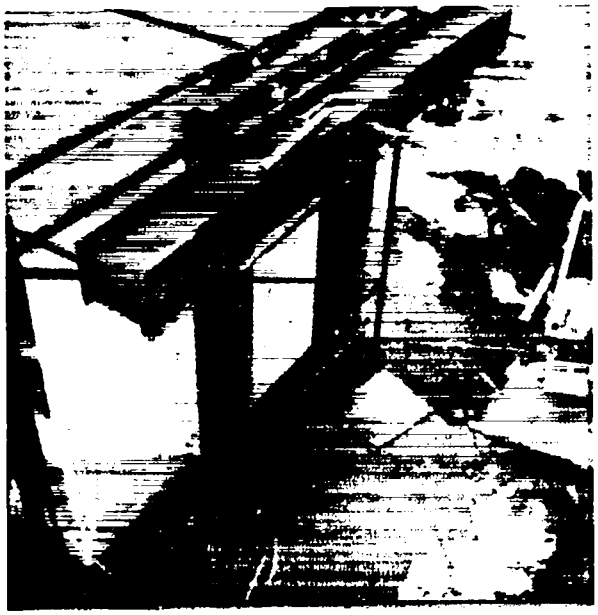

(b)

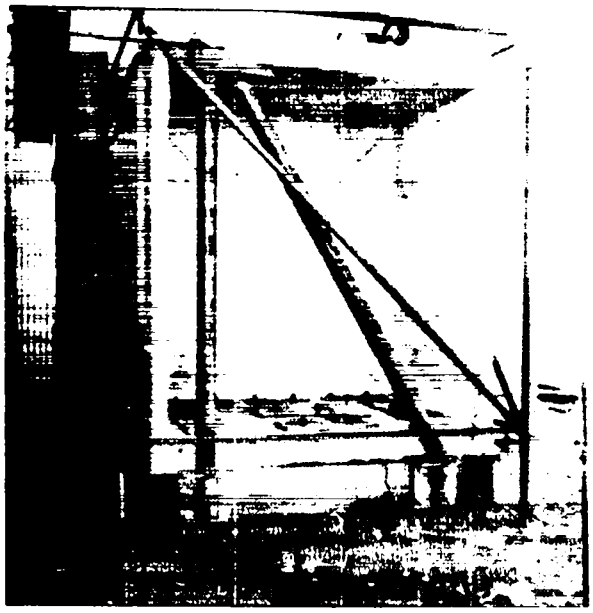

(c)

Fig. 8. Static load frame details.

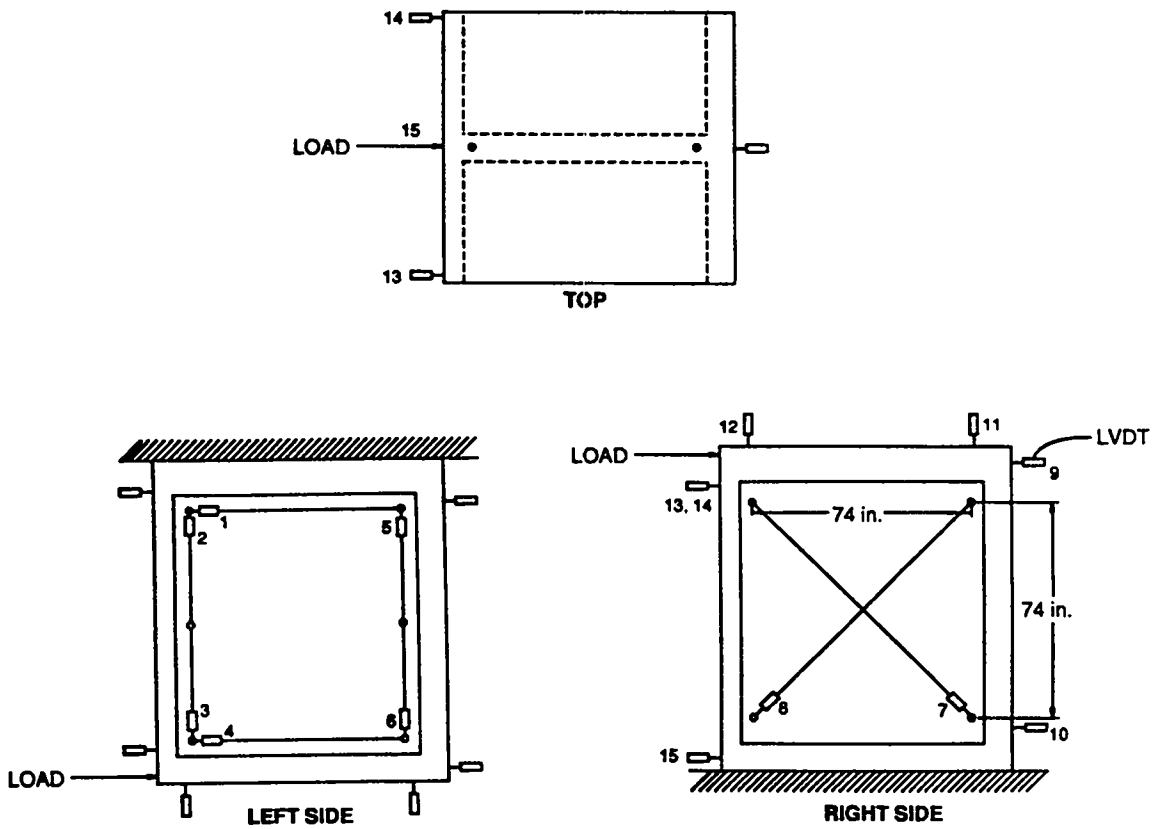

Fig. 9. Locations of the linear voltage differential transformer displacement measurements taken during the static testing of the TRG-3 structure.

It is noted in Fig. 9 that a 74-in. x 74-in. segment of the shear wall is covered by the LVDT gaging.

Using an average shear strain determined from the above equation, the shear deformation, ΔS, for the gaged area may be calculated as

$$\Delta S = H \gamma_{avg} \quad ,$$

where H is the height of the gaged area, in this case 74 in. (Fig. 9). To calculate the total deformation for the model and then the model spring constant, ΔS must be corrected with two factors. One is a correction for the height of the model being greater than the internal gaged area. A linear factor based upon the ratio of the model height to gaged height was used here, i.e., 106 in./74 in.

The second correction factor is used to include the bending deformation. The deformation as calculated above, ΔS, is only shear deformation. The total deformation will have a component caused by bending. Ideally, LVDTs 1 -- 6 were to give data from which the total deformation could be calculated. However, the deformations at these points were too small to be resolved with the transducers used, so the bending component of deformation was based upon analysis and a subsequent TRG test. The analysis, using a finite element model of a similar structure but having 6-in.-thick walls, but also having an aspect ratio of one, showed that the bending deformation is about 12% to 15% of total deformation. The subsequent test results of a later TRG test gave values of 10% to 20%. A value of 12% was used in the data reduction here.

The maximum internal LVDT reading was 0.0018 in. at location 8, which illustrates the resolution problem at low-load levels. However, this signal was linear with force, and a study of the results of the four tests indicated that the data from transducers 7 and 8 were reliable. Using these data and the data reduction method described, the spring constant for the TRG-3 structure was determined to be $4.4 \times 10^{+6}$ lb/in.

C. Tests Conducted at CERL

The TRG-3 structure was loaded (using a mobile crane) on a commercial low-boy truck on January 2, 1986, for shipment to CERL. No instrumentation was used during shipping. The structure was visually inspected after off-loading at CERL and no damage to the shear wall was observed. However, the base slab shows some areas of visible cracking near the edges that occurred because of the truck bed flex over the axle. These areas were not judged to be significant with respect to the structural integrity of the model. During the week of January 6, 1986, the structure was suspended from the CERL crane using nylon straps and "free-free" modal testing was carried out using a portable shaker and random force excitation (see Fig. 10). In these tests, coherence at lower frequencies was good, and the modal analysis gave satisfactory results. The first mode was found to be a torsional mode with a frequency of 29 Hz. The second mode was the shear-bending mode with a frequency of 75 Hz. The details of the methods of modal analysis data reduction are given in Ref. 9.

The structure was next bolted to the CERL test table and two 6-in.-thick steel plates were bolted to the top of the structure. Figure 11 indicates how

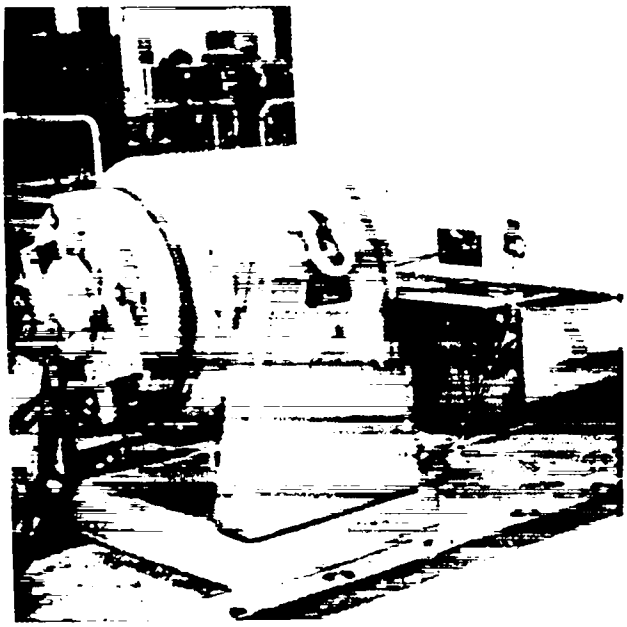

(a)

Modal shaker

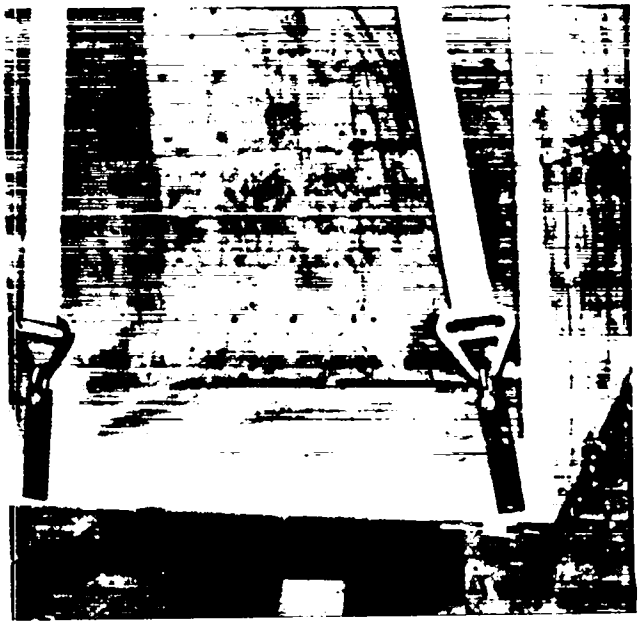

(b)

Nylon strap suspension system

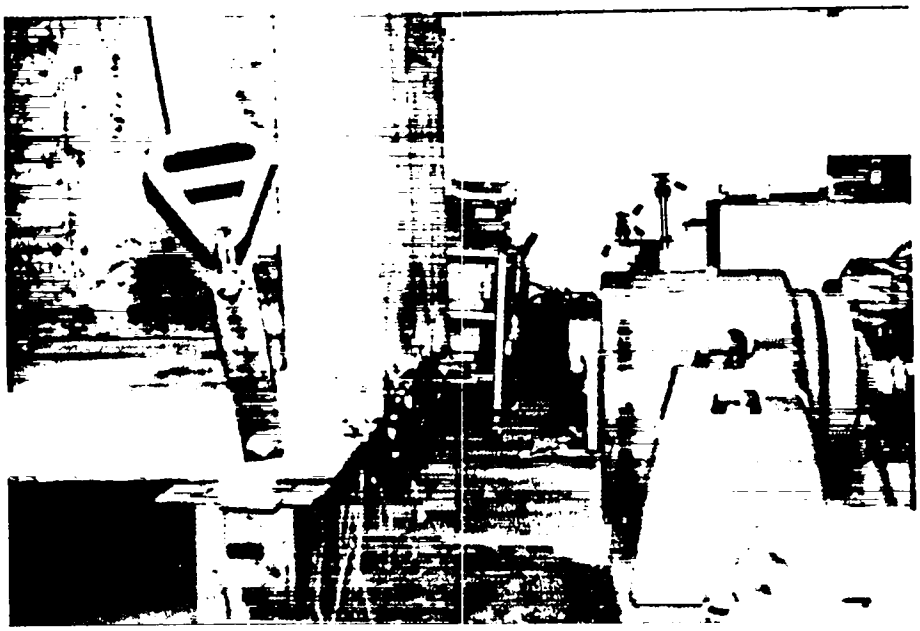

(c)

Stinger and force link

Fig. 10. Modal testing in the free-free mode at CERL with the structure suspended from nylon straps.

results. The first mode was found to be a torsional mode with a frequency of 29 Hz. The second mode was the shear-bending mode with a frequency of 75 Hz. The details of the methods of modal analysis data reduction are given in Ref. 9.

The structure was next bolted to the CERL test table and two 6-in.-thick steel plates were bolted to the top of the structure. Figure 11 indicates how the structure was attached to the shake table. Accelerometers were mounted on the structure at the locations indicated in Fig. 12.

A low-level haversine pulse was used to excite the structure over a wide frequency range for diagnostic testing. This single haversine pulse was used instead of the low-level, broad-band noise signal used in previous tests in an attempt to limit damage to the structure due to numerous load cycles. The

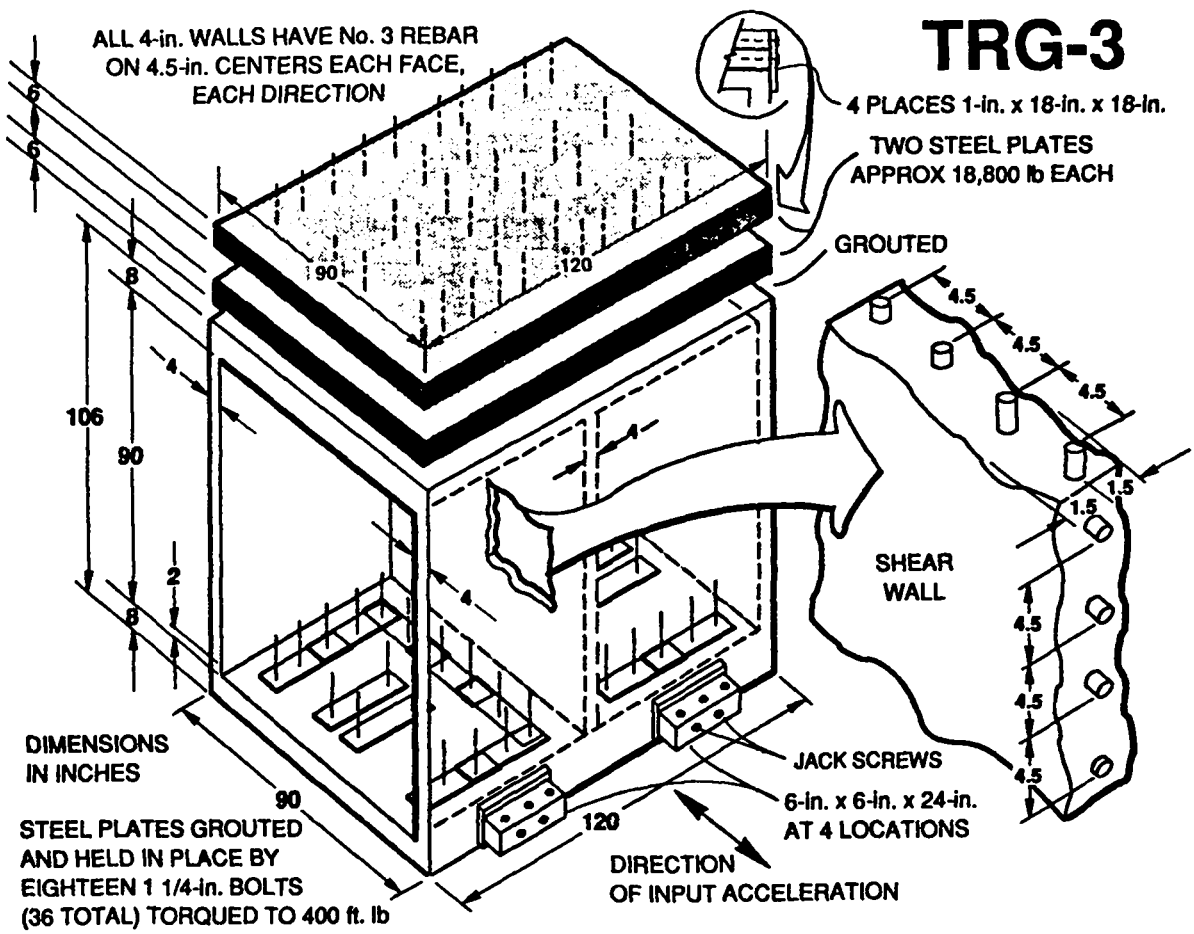

Fig. 11. Method used to attach TRG-3 to CERL shaker.

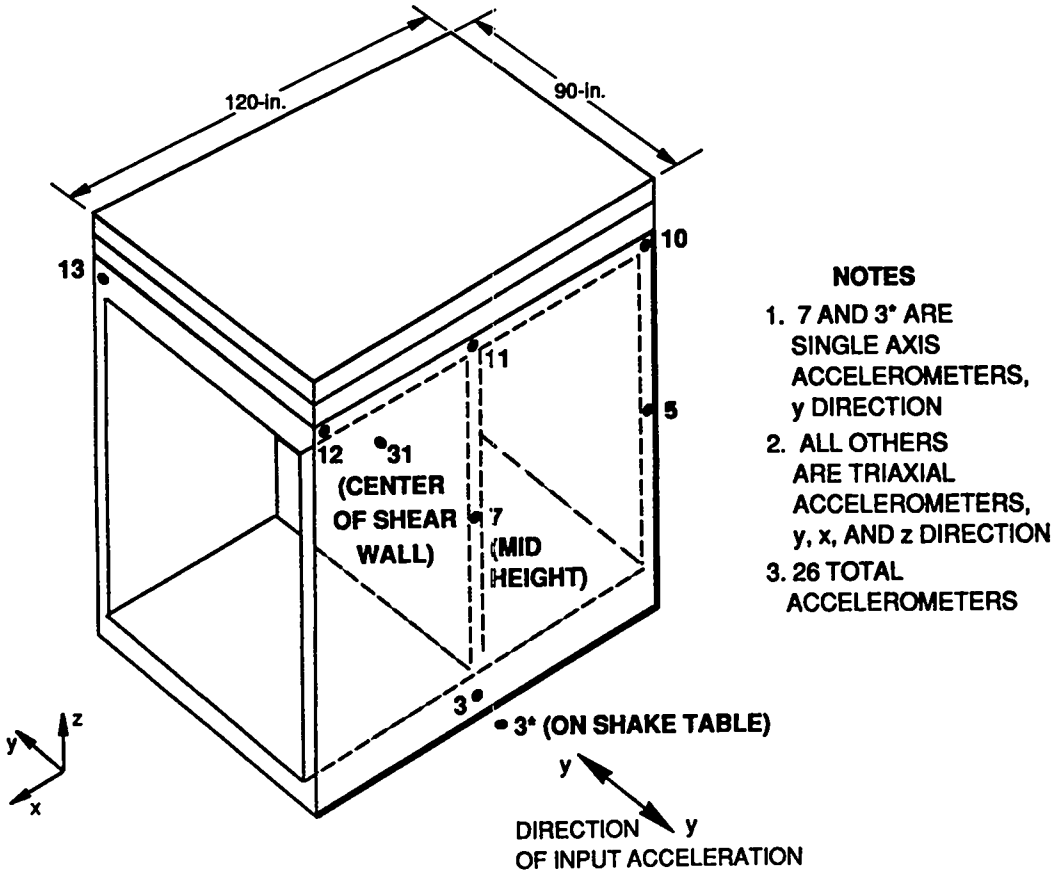

Fig. 12. Schematic showing the locations of the accelerometer on the TRG-3 structure.

control signal was a pure haversine; however, because of control system distortion and feedback from the structure, the actual test pulse applied to the base of the structure had the shape shown in Fig. 13.

The simulated seismic pulse used in the TRG-3 tests was the base line corrected version of the 1940 El Centro, N-S accelerogram (previously used in the TRG-1 test) time scaled by a factor of 5. The complete test sequence for TRG-3, together with the sequence followed in the testing of TRG-1, is given in Table IV.

All of the data (from the 26 accelerometers) were recorded on magnetic tape for later digitization and analysis.

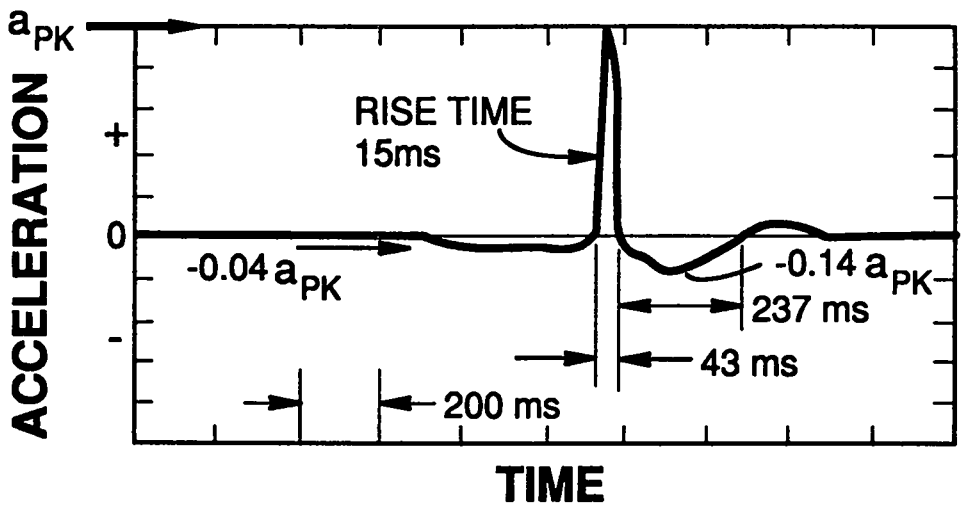

Fig. 13. Haversine pulse used in the TRG-3 test.

III. THEORETICAL ANALYSIS OF THE TRG STRUCTURE

The various tests conducted to evaluate the TRG structures (static, modal, and simulated seismic) have been described in the preceding section. The second but integral part of this evaluation consisted of theoretical analysis. Three methods of analysis were used in order to cover the various approaches that might be used in the design of this type of structure and to point out the consequences (in terms of predicted stiffness and modal frequencies) of each method of analysis.

A. Design Method

This is the method actually used in the design of the structure tested in this program (TRG-1 and TRG-3) and is the method that has been most used by architectural/engineering firms for the design of existing nuclear plant structures of this type. The assumptions for this method are as follows:

1. assume an uncracked concrete cross section;
2. use the method of transformed sections to transform steel area to concrete and compute the transformed bending area moment of inertia for the cross section; this step may or may not be done by an architectural engineering firm;
3. use the strength-of-materials approach to compute the stiffness,

TABLE IV

TRG TEST SEQUENCE

Test	TRG-1 (1/4 Scale)	TRG-3 (Prototype)
1. No mass added, free-free modal	1. Structure on foam pad at construction site; ± 25 lb force shaker, good results f_1 = 112.5 Hz torsion f_2 = 307.5 Hz shear/bending	1. Structure on foam pad at construction site, ± 300 lb force shaker, poor results f_1 not determined f_2 not determined
2. Low-level monotonic test	2. At construction site measured tangent stiffness at origin $K_0 = 0.75 \times 10^6$ lb/in.	2. At construction site measured tangent stiffness at origin $K_0 = 4.4 \times 10^6$ lb/in. (poor resolution)
3. No mass added, free-free modal (repeat of test 1)	3. After transporting to test site (K site, Los Alamos) f_1 = 107.5 Hz torsion f_2 = 293.8 Hz shear/bending	3. After transporting to test site (CERL), structure suspended from crane f_1 = 29 Hz torsion f_2 = 75 Hz, shear/bending
4. No mass added, fixed-free modal (base clamped to shaker table)	4. At test site, good base fixity with table locked, f_1 = 221.2 Hz, shear/bending	4. No comparable test on TRG-3 because CERL table cannot be locked
5. No mass added, low-level base input	5. At test site, ± 0.5 g random table input f_1 = 192.6 Hz, shear/bending	5. No comparable test on TRG-3
6. Mass added, low-level base input	6. At test site 575 lb added, ± 0.5 g random table input f_1 = 76.6 Hz, shear/bending	6. At CERL, 37,600 lb added, haversine pulse at base a_{pk} (g) f_1 (Hz) shear/bending 0.2 9.5 0.5 9.0
7. Repeat of No. 5	7. Mass removed and repeat No. 5 to check for damage f_1 = 186.9 Hz shear/bending	7. No comparable test on TRG-3
8. Mass added, simulated seismic sequence (time scaled 1940 El Centro, N-S)	8. El Centro time scaled by a factor of 20 a. Seismic, a_{pk} = 0.5 g b. Random, ± 0.5 g c. Seismic, a_{pk} = 1 g d. Random, ± 0.5 g e. Seismic, a_{pk} = 2 g f. Random, ± 0.5 g g. Seismic, a_{pk} = 4 g h. Random, ± 0.5 g i. Seismic, a_{pk} = 5 g j. Random, ± 0.5 g k. Seismic, a_{pk} = 8.9 g (Visable cracks) l. Random, ± 0.5 g m. Seismic, a_{pk} = 1 g n. Random, ± 0.5 g o. Seismic, a_{pk} = 15 g (Structure failed)	8. El Centro time scaled by a factor of 5 a. Seismic, a_{pk} = 0.25 g b. Seismic, a_{pk} = 0.38 g c. Haversine, a_{pk} = 0.5 g d. Seismic, a_{pk} = 0.5 g e. Seismic, a_{pk} = 0.65 g f. Seismic, a_{pk} = 0.75 g g. Haversine, a_{pk} = 0.5 g h. Seismic, a_{pk} = 1.0 g i. Haversine, a_{pk} = 0.5 g j. Seismic, a_{pk} = 1.5 g At this acceleration level the hydraulic system shut down probably due to uncontrollable overturning moment. k. Five additional seismic tests were attempted (with peak levels up to 3.5 g), but in every case the test facility malfunctioned and the desired seismic pulse was not reproduced.

4. assume the top and bottom concrete slabs are rigid compared to the "beam" cross section and compute the effective

$$\text{Mass} = M_{ADDED} + M_{SLAB} + M_{DISTRIBUTED};$$ and

5. assume that the base is fixed.

The sample calculations involved in this method are given in Appendix A.

B. Structural Dynamics Method

The engineering mechanics specialist might approach this problem from an energy method point of view and use Hamilton's principle and shape functions to obtain the best single degree-of-freedom representation possible for the TRG-3 structure and its base connections. The details are summarized in Appendix B, and the interested reader can obtain the theory from Refs. 10 and 11.

C. Finite Element Method

The finite element method of analysis has found increasing use in the design of nuclear power plant structures. Hence, it has been used here to analyze the TRG structures. Two cases are considered:

1. fixed base,
2. base connection effects modeled.

The ABAQUS finite element code was used with shell elements representing the structure and a smeared rebar option combined with the concrete material model to represent the material. The calculations are totally elastic. The structure was represented using the quarter model mesh shown in Fig. 14 with the appropriate symmetry boundary conditions for the vibration modes of interest.

The results of these computations using all three methods and with $E = 3.5 \times 10^6$ lb/in. $\left(57{,}000 \sqrt{f'_c}\right)$ are given in Table V.

Clearly, the method of analysis chosen has a considerable effect on the computed stiffness and hence on the predicted modal frequency. Which method gives the "correct" or "best" solution is of course unknown at this point. In the following section we will examine all of the available experimental data to determine the actual response of the TRG structure.

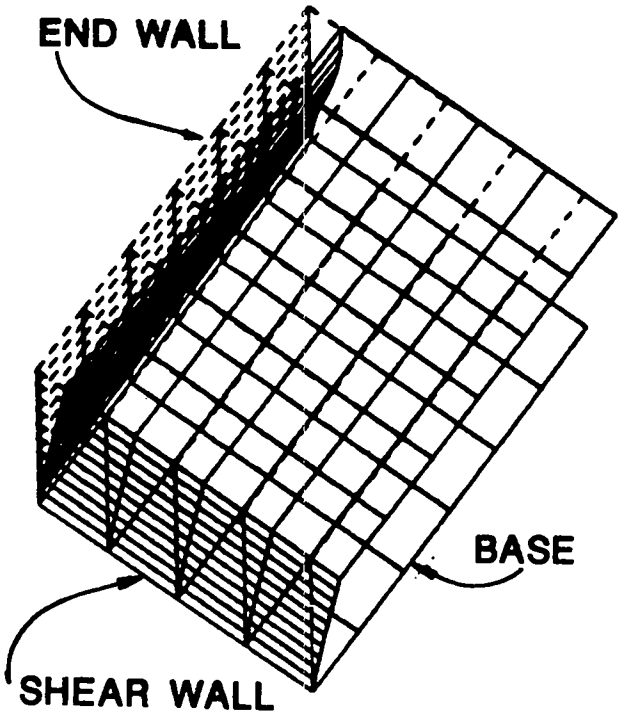

Fig. 14. One-quarter model finite element mesh used for finite element calculations.

IV. COMPARISON OF EXPERIMENTAL RESULTS FROM TRG-1 AND TRG-3

As pointed out in a previous section of this report, the TRG structure was subjected to a series of tests that were specifically designed to determine the "as-constructed" stiffness and modal frequency and to track changes in those two values as the structure was subjected to progressively larger loads. See Table IV for the test sequence. The 1/4-scale microconcrete model (TRG-1) of this prototype structure (TRG-3) had previously been tested in essentially the same sequence. Hence, it is now possible to compare the values for stiffness and modal frequency measured on the TRG-3 structure and the scale model predictions.

Table VI gives the values of modal frequencies or stiffness for the static tests measured during the various tests on both the TRG-1 and TRG-3 structures. In addition, the values predicted for the prototype (TRG-3) from the model (TRG-1) results are given.

TABLE V

COMPARISON OF THREE METHODS OF ANALYSIS
(TRG-3, using $E_c = 3.5 \times 10^6$ psi
and $E_{STL} = 30 \times 10^6$ psi)*

Method	Stiffness K (lb/in.)	First Mode Frequency f_1 (Hz)
1. Design method	5.0×10^6	31.8
2. Structural dynamics method	2.76×10^6	18.9
3. Finite element method		
a. Base fixed	4.04×10^6	29.0
b. Base bolts modeled as springs	2.71×10^6	22.7

* Values for TRG-1 are values shown for TRG-3 divided by 4. Frequency, f, values for TRG-1 are values shown for TRG-3 multiplied by 4.

Examination of the data obtained from the TRG-1 (1/4-scale model) tests indicates that reduction in stiffness (as shown by reduction in modal frequency) was progressive during the test sequence. This observation is consistent with the results previously observed during the tests on other model structures.[2,3] The reduction of the shear/bending modal frequency between the test at the construction site, Test No. 1, and the test at the shaker test site, Test No. 3, (from 307.5 Hz to 293.8 Hz) indicates that some damage may be caused by handling. This reduction is relatively small; however, precisely this reduction in modal frequency corresponds to a reduction in shear/bending stiffness of

$$\frac{K_2}{K_1} \alpha \left(\frac{f_2}{f_1}\right)^2 = \left(\frac{293.8}{307.5}\right)^2 = 0.91 \quad ,$$

or 91% of the initial value. However, from the first simulated seismic test (No. 8a, $a_{PK} = 0.5$ g) to the test after which concrete cracking was visually observed (8K, $a_{PK} = 8.9$ g), the shear/bending stiffness is reduced to

$$\frac{K_f}{K_i} \propto \left(\frac{f_f}{f_i}\right)^2 = \left(\frac{45}{75}\right)^2 = 0.36 \quad ,$$

or 36% of its value at the beginning of the seismic test series.

TABLE VI

MEASURED AND PREDICTED MODAL FREQUENCIES AND STIFFNESSES

	TRG-1	TRG-3	
Test	Measured	Measured	Predicted by scaling
1. Modal test, free-free	$f_1 = 112.5$ Hz, torsional $f_2 = 307.5$ Hz, shear/bending	No usable data obtained at Los Alamos before shipping	$f_1 = 112.5/4 = 28.1$ Hz $f_2 = 307.5/4 = 76.9$ Hz
2. Low-level static, base fixed	Tangent modulus at origin $K_0 = 0.75 \times 10^6$ lb/in.	Tangent modulus at origin $K_0 = 4.4 \times 10^6$ lb/in. (poor resolution)	$K_0 = (0.75 \times 10^6) \times 4$ $= 3.0 \times 10^6$ lb/in.
3. Modal test free-free	$f_1 = 107.5$ Hz, torsional $f_2 = 293.8$ Hz, shear/bending	$f_1 = 29$ Hz, torsional $f_2 = 75$ Hz, shear/bending	$f_1 = 107.5/4 = 26.8$ Hz $f_c = 293.8/4 = 73.4$ Hz
4. Modal test, fixed-free	$f_1 = 221.2$ Hz, shear/bending	None	
5. No top mass, low-level base input	$f_1 = 192.6$ Hz, shear/bending	None	
6. Top mass added, low-level base input	$f_1 = 76.6$ Hz, shear/bending	at 0.2 g pk base input $f_1 = 9.5$ Hz, shear/bending at 0.5 g pk base input $f_1 = 9.0$ Hz, shear/bending	$f_1 = 76.6/4 = 19.2$ Hz
7. Repeat of No. 5	$f_1 = 186.9$ Hz, shear/bending	None	
8. Simulated seismic test sequence top mass added, base input	at $a_{PK} = 0.5$ g, $f_1 = 75$ Hz at $a_{PK} = 8.9$ g (cracking) $f_1 = 45$ Hz	at $a_{PK} = 0.25$ g $f_1 = 9.4$ Hz at $a_{PK} = 2.5$ g $f_1 = 8.1$ Hz	at $a_{PK} = 0.5/4 = 0.125$ g $f_1 = 75/4 = 18.8$ Hz at $a_{PK} = 8.9/4 = 2.2$ g $f_1 = 45/4 = 11.3$ Hz

Examination of the data (in Table VI) taken from the TRG-3 tests shows that during the simulated seismic testing there is a progressive reduction in stiffness:

$$\frac{K_f}{K_i} \propto \left(\frac{f_f}{f_i}\right)^2 = \left(\frac{8.1}{9.4}\right)^2 = 0.74$$

or K_f = 74% of K_i.

This reduction in stiffness for TRG-3 during the seismic test sequence is not as great as was observed in the TRG-1 structure (or as in other structures previously tested).[2,3] It is impossible to say whether or not this discrepancy is caused by a failure to properly model concrete material properties and behavior when microconcrete is used to model "real" concrete. It is impossible to know the causes for the discrepancy because the seismic loading function was not properly modeled between model (TRG-1) and prototype (TRG-3) seismic tests. Especially in the TRG-3 tests, the frequency content of the input signal was greatly distorted at the higher peak acceleration seismic tests, and, as a result, these tests were not as severe as the peak "g" level would indicate.

The low-level (40 psi average base shear) static test (item No. 2, Table VI) and the free-free modal test (item No. 3, Table VI) indicate that the microconcrete TRG-1 structure is a reasonable model of the TRG-3 structure. Specifically, since stiffness (K) scales by the length scale (N_K = 4 in this case) and frequency (f) scales by the reciprocal of the length scale (N_f = 1/4 in this case),* the values predicted for the prototype by the model are as shown in the fourth column of Table VI.

Comparing the values of K and f_1 measured during low-load-level tests on TRG-3 with the values predicted by scaling, we conclude that the microconcrete model underpredicts the prototype stiffness, i.e., from the low-level static test

$$\frac{K_{MEAS}}{K_{SCALED}} = \frac{4.4}{3.0} = 1.47 ,$$

---

* This scaling assumes that the modulus (E) is the same for both model and prototype. Taking E as $57{,}000\sqrt{f_c}$, we have $E_M = E_p = 3.5 \times 10^6$ lb/in. (Table II).

and from the free-free modal test

$$\frac{K_{MEAS}}{K_{SCALED}} = \left(\frac{f_{MEAS}}{f_{SCALED}}\right)^2 = \frac{75.0}{73.4} = 1.04 \quad .$$

The first number is disappointing; it suggests that the low-load-level stiffness of the prototype predicted from the scale model is only 68% $\left(K_{SCALED}/K_{MEAS} = 1/1.47\right)$ of the actual measured value. However, it should be remembered that the resolution of the data to obtain the initial stiffness (slope at the origin of the load deflection curve) as measured on the prototype is poor; see pages 14 through 17 for a discussion of these problems. In any case, it is clear that the microconcrete model does <u>not</u> underpredict the initial structural stiffness. Thus, microconcrete cannot be used to explain the discrepancy between experimental and theoretical values of stiffness noted in our previous tests on microconcrete models of various Category I structures.[2,3]

The second number $\left(K_{MEAS}/K_{SCALED} = 1.04\right)$, which is the result of dynamic tests in which the modal frequencies can be measured with better precision, suggests that at low-load levels the microconcrete model predicts the prototype's effective stiffness very well.

With steel plates attached to the top of the TRG structures, and the structures bolted to the shake table (tests No. 6 and No. 8, Table VI), the structures are configured for the simulated seismic testing. In this condition the TRG-1 structure was found to have a first mode frequency (shear/bending) of 76.6 or 75.1 Hz (see tests 6 and 8, Table VI). Having shown in the preceding paragraph that, at low-load levels, the TRG-1 structure is a good model of the TRG-3 prototype, we can scale these results to predict the first mode frequency of the TRG-3 under the same mounting and load condition (i.e., base fixed to shaker table, input acceleration pulse at base).

Thus,

$$f_{1_{TRG-3}} = \frac{f_{1_{TRG-1}}}{4} = \frac{75.1}{4} = 18.8 \text{ Hz} \quad .$$

The measured value of the TRG-3's first mode frequency was 9.5 Hz (test 8a, Table VI). Clearly, in this condition, the TRG-3 structure is poorly modeled

by the TRG-1 model, and the reason or reasons for this situation must be investigated.

We can check the response of a structure by using vibration theory to predict its first mode frequency in this test condition from previous test results. We can thus check the response of the TRG-1 structure.

From test No. 5, with the base fixed but with no additional mass added, f_1 was found to be

$$f_1 = 192.6 \text{ Hz} \quad .$$

Since modal frequency is inversely proportional to mass,

$$f_{1_{\substack{\text{MASS}\\\text{ADDED}}}} = f_{1_{\substack{\text{NO ADDED}\\\text{MASS}}}} \times \sqrt{\frac{M_{\text{TEST NO. 5}}}{M_{\text{TEST NO. 6}}}} = 192.6 \times \sqrt{\frac{25.3}{122.7}} = 87.5 \text{ Hz} \quad .^{*}$$

Then the measured value of first mode frequency (f_1 = 76.6 Hz) is

$$\frac{f_{1_{\text{MEAS}}}}{f_{1_{\text{COMP}}}} = \frac{76.6}{87.6} \quad ,$$

or

$$f_{1_{\text{MEAS}}} = 0.87 \; f_{1_{\text{COMP}}} \quad .$$

We attribute this relatively small difference to the progressive reduction in stiffness from test to test on the TRG-1 structure and, hence, we believe that the measured value of f_1 represents the actual modal frequency of this structure in shear/bending on a fixed base.

---

* See Appendix A for the computation of masses. Values of masses given in Appendix A are for TRG-3; however, the <u>ratio</u> of masses is the same in TRG-1 as in TRG-3.

We can also check the response of the TRG-3 structure in the same way. However, because this structure was not tested in the "no added mass, base fixed" condition (test No. 5, Table VI), we must compute the expected value of f_1 for test No. 6 (mass added/base fixed) from the value measured in test No. 3 (no mass added, free-free modal). We perform this computation as follows:

In test No. 3, the shear/bending mode for free-free boundary conditions, f_2, was found to be

$$f_{S/B} = 75 \text{ Hz.}$$

The expected shear/bending modal frequency with fixed-free boundary conditions and additional mass added is

$$f_{S/B_{FIX-FREE}} \times \sqrt{\frac{K_{FIX-FREE}}{K_{FREE-FREE}} \times \frac{M_{FREE-FREE}}{M_{FIX-FREE}}} \quad .$$

We have

$$f_{S/B_{FIX-FREE}} = 75 \times \sqrt{\frac{5.09}{11.61} \times \frac{22.4}{122.7}} = 21 \text{ Hz}^* \quad .$$

However, the actual measured value of the shear/bending modal frequency of the TRG-3 structure in this condition was $\left(f_1 = f_{S/B} = 9.5 \text{ Hz}\right)$; thus,

$$f_{1_{MEAS}} = \frac{9.5}{21.0} f_{1_{COMP}} = 0.45 \, f_{1_{COMP}} \quad .$$

We believe that this is clear evidence that in this test condition it is the TRG-3 structure that is responding in a manner that was not anticipated, nor adequately understood, or accounted for. Two possibilities suggest themselves. First, the TRG-3 structure may have experienced considerably more

---

* *See Appendix A* for computation of masses and stiffnesses.

relative damage than did the TRG-1 structure when the top mass was added, the base was bolted to the shaker test table, and the fixed base input was applied. Second, the TRG-3 structure may undergo significant rigid body rotation when tested in this configuration. This rotation would result in an observed modal frequency lower than the value that would result from pure shear/bending about a fixed base, and as a result, it could not be used to compute the effective shear/bending stiffness without further analysis.

We investigated this second possibility by using the computer model of the system shown in Fig. 15. This model includes torsional (K_R) vertical (K_V), and translational (K_1) springs and dampers to allow for rotation, vertical and translation motion of the structure relative to the shake table. The details of this investigation are given in Appendix C. The results of

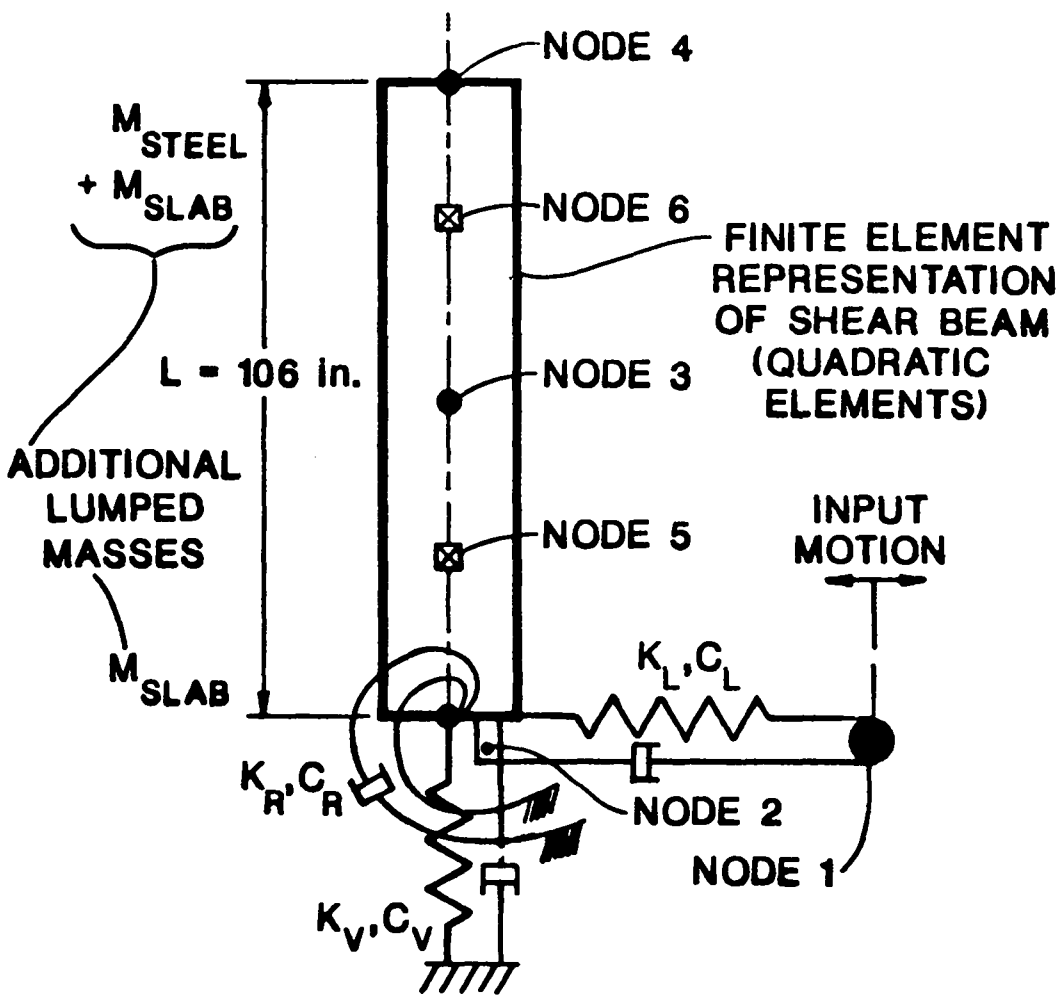

Fig. 15. Computational model used to study the base connection effects.

this investigation may be summarized as follows. The time history data taken from two of the accelerometers for the fourth haversine base pulse applied to the structure are shown plotted in Fig. 16. The programmed shaker input pulse is also shown on this figure. Figure 17 shows the transfer function of the top accelerometer to the base slab accelerometer for the records of Fig. 16. This transfer function clearly indicates a strong natural mode at about 7.7 Hz which corresponds to the frequency that can be obtained by "counting response cycles" on Fig. 16. The question the computer model tried to address is, "how is natural frequency influenced by base connections?" A number of computer

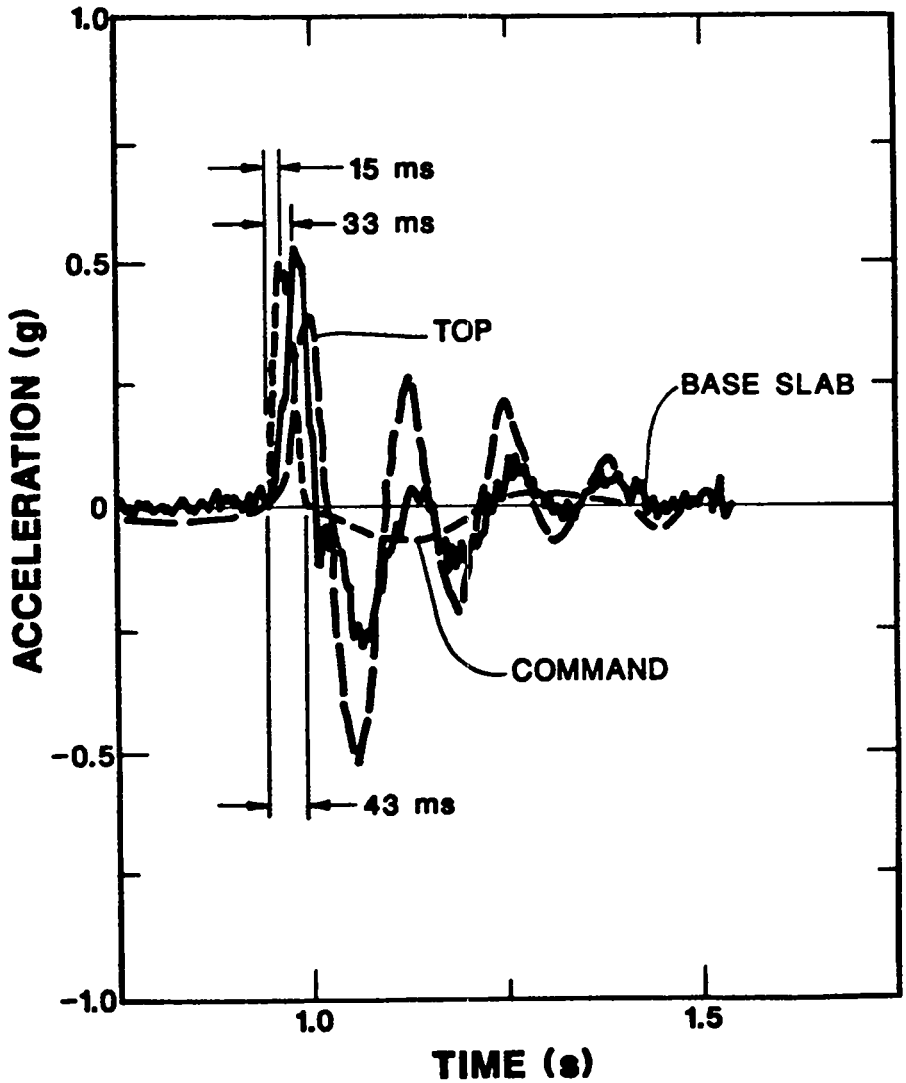

Fig. 16. Command signal, base and top accelerometer records from haversine pulse applied to TRG-3 at CERL.

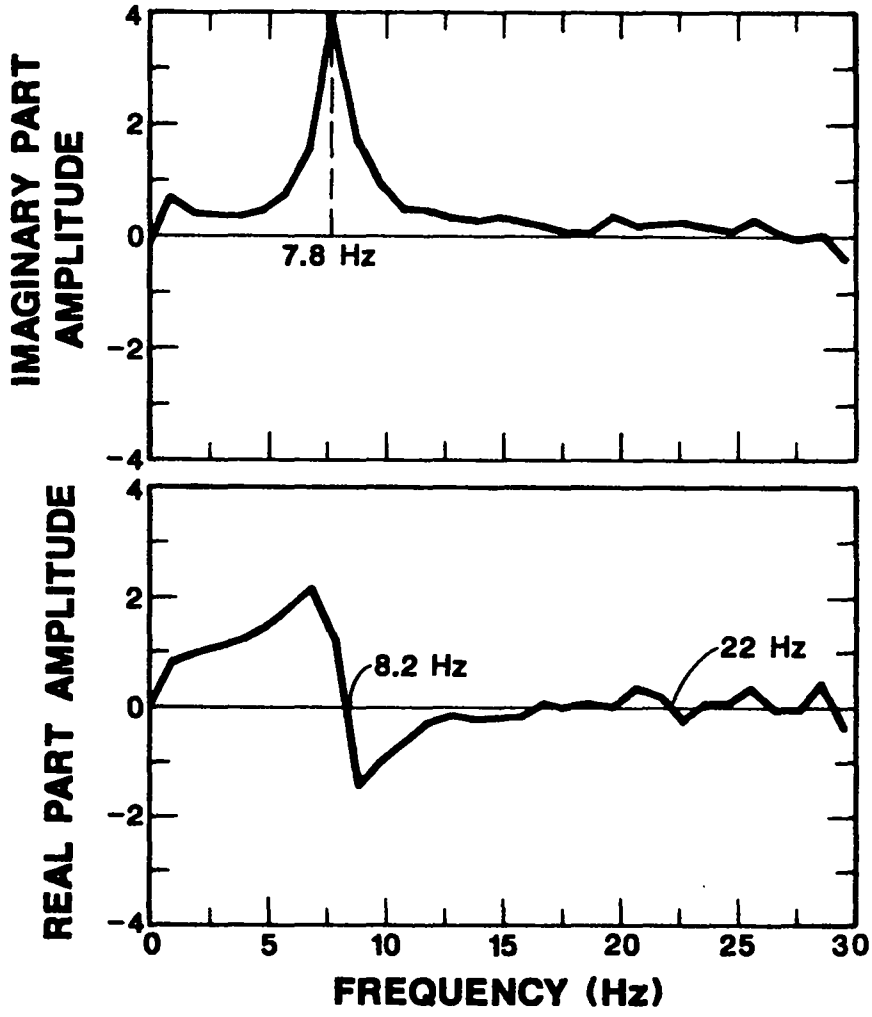

Fig. 17. Real and imaginary parts of the transfer function for the top slab accelerometer to the base for the time histories of Fig. 16.

runs were made to study this question. Figures 18-21 illustrate the results of one run that seems to best simulate the data. To obtain this "match," the structural stiffness of the model of Fig. 15, K_s, had to be lowered to 3×10^5 lb/in. (from $K_{THEORY} = 3.15 \times 10^6$ lb/in.), a factor of about 10. Other selections of structural connection springs and combinations of base connection springs will also give an approximate "match," because they all represent a factor of 6 or better reduction in stiffness.

To illustrate the difference, the structural stiffness can be set to a theoretical value and the base connection springs adjusted to give a first mode frequency of about 7.7 Hz. Calculated transfer functions of top to base

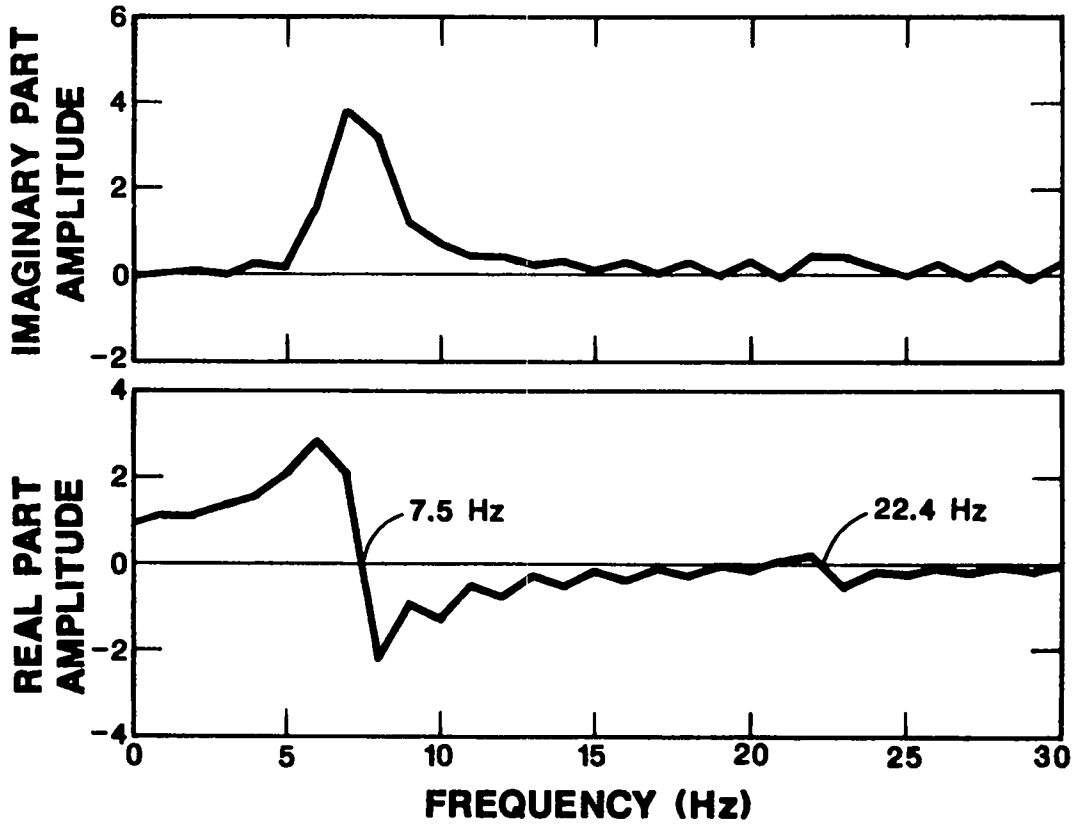

Fig. 18. Transfer function computed from the time history of node 4 to node 2 for the computational model of Fig. 15.

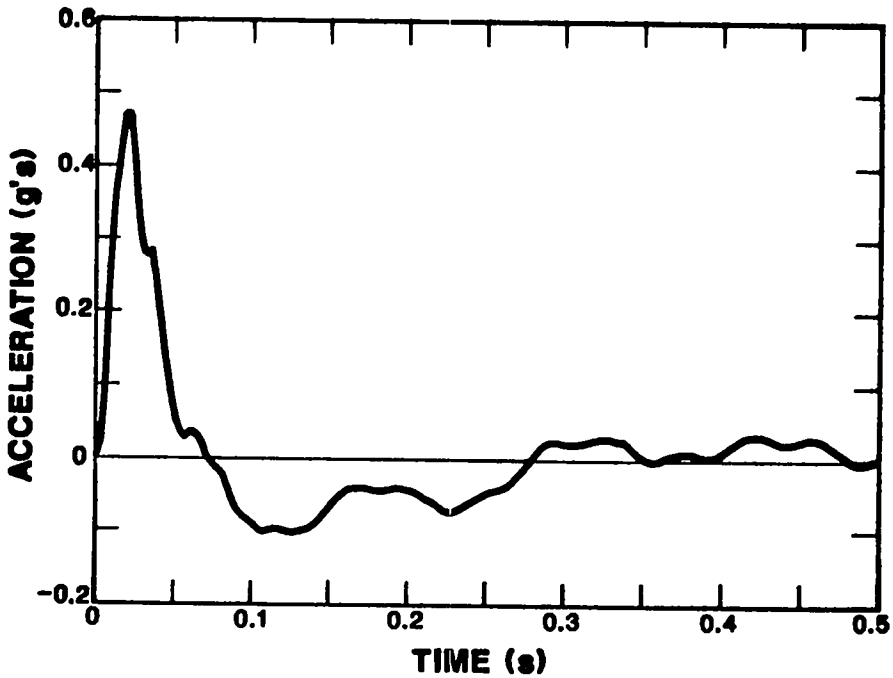

Fig. 19. Time history of node 2 for the computer model of Fig. 15.

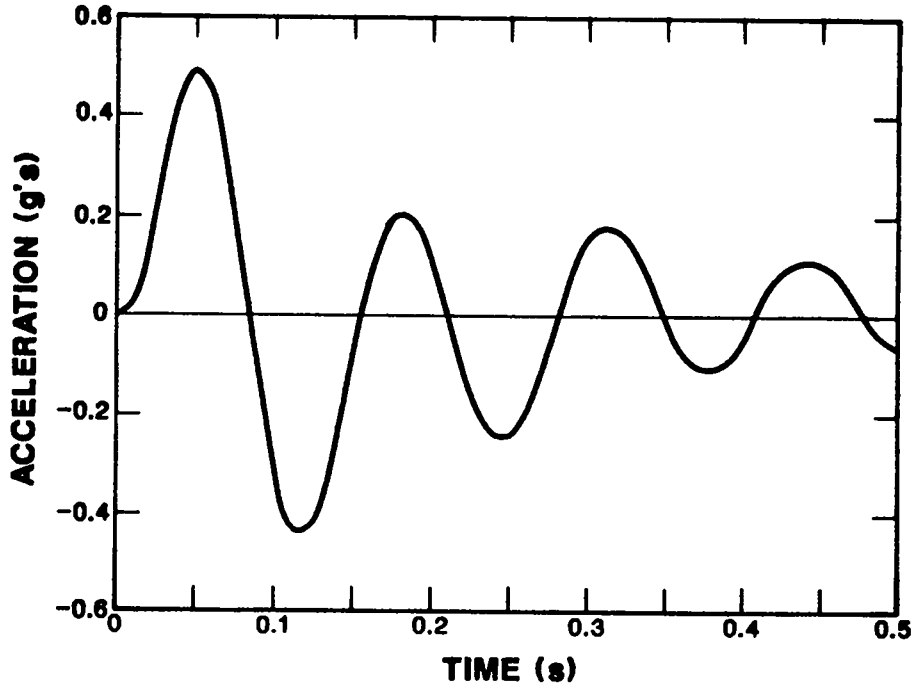

Fig. 20. Time history of node 4 for computer model of Fig. 15. $K_S/K_T \approx 0.1$.

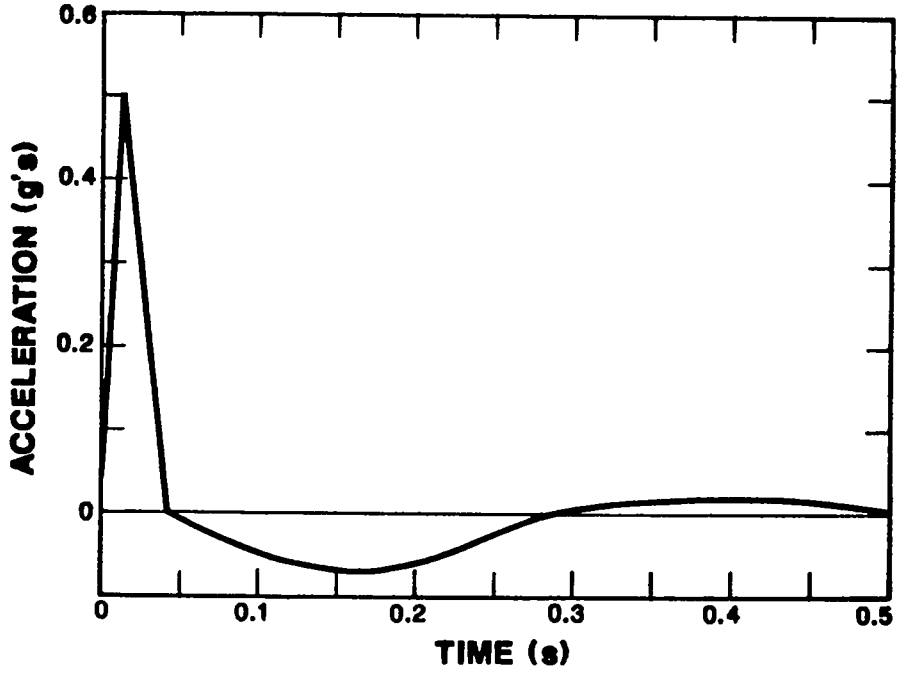

Fig. 21. "Command" signal applied to node 1 model of Fig. 15.

from the analytical model will again be similar to those from the measured data as shown in Figs. 22 and 23. However, calculated time histories of the base and top nodes are dramatically different from measured base and top response as shown in Figs. 24 and 25.

The conclusion from the analytical study is that (1) base connections can indeed influence the model's response, but not significantly enough to change the interpretation of the result, (2) the stiffness of TRG-3, when subjected to the initial base input haversine pulses on the CERL table, was down by at least a factor of 4, as initially reported.

V. COMPARISON OF THEORETICAL AND EXPERIMENTAL RESULTS

Having gained some insight into the results of the TRG-3 structure tests by comparison with TRG-1 (model) test results, we now turn to the comparison of experimentally determined values of shear/bending stiffness with theoretically computed values. In the static tests, the stiffness is obtained from displacement measurements and geometrical computations. In the dynamic tests, the stiffness is inferred from the measured frequencies. Therefore, it must be remembered that the experimentally determined values of stiffness are not measured directly. As was previously pointed out in the static test of TRG-3, the displacement measurements are suspect because of poor resolution of the LVDT gauges. In the dynamic tests (modal and simulated seismic), the modal frequencies can be determined with better precision; however, the calculation of stiffness from modal frequency involves vibration theory and the associated assumptions concerning the actual effective mass, the actual boundary conditions, etc. In this case, the experimentally determined stiffness (K) is calculated from the measured modal frequency (f) using the equation for a single degree of freedom system:

$$K = (2\pi f)^2 M \quad .$$

The appendices show the way in which the effective mass (M) is calculated. The values of M used in the calculations for the various boundary condition cases (free-free; fixed-free, no added mass; and fixed-free, added mass) are given in Table VII. The computation of theoretical values of stiffness has been discussed in Section III of this report and the details are given in Appendices A

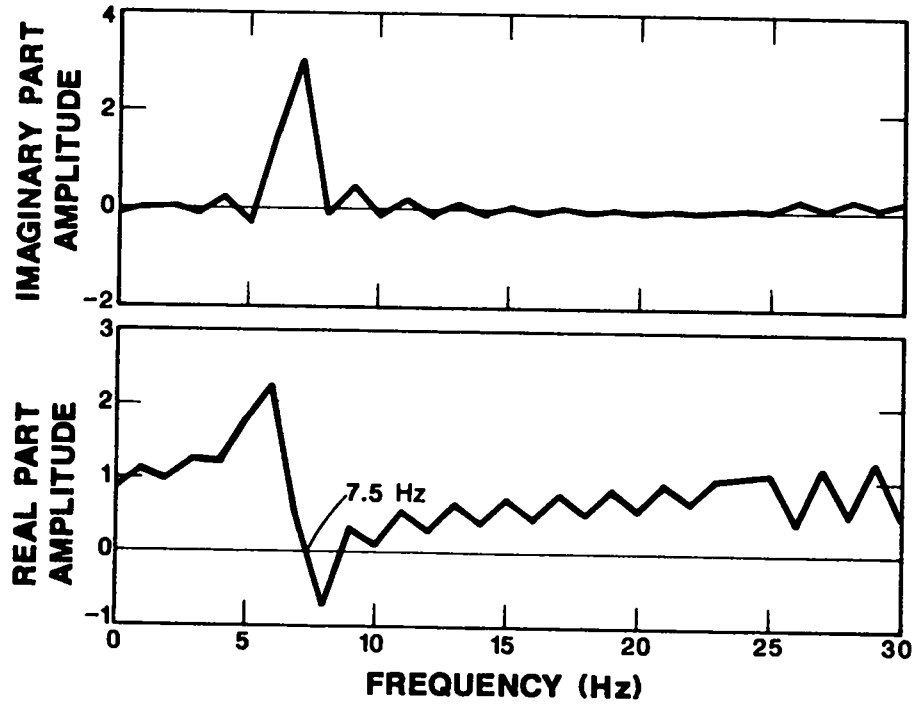

Fig. 22. Transfer function of node 4 to node 2 for model of Fig. 15 with $K_{STRUCTURAL} = K_{THEORY}$ and base connection springs lowered to give 7.7 Hz.

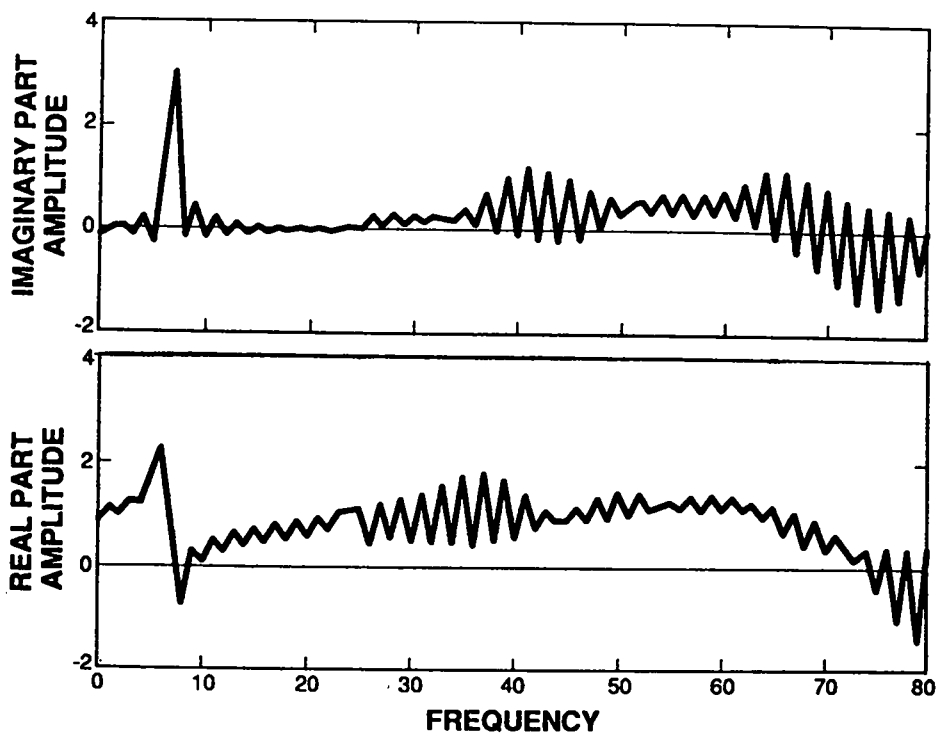

Fig. 23. Transfer function of node 4 to node 1 for model of Fig. 15. $K_{ST}/K_T \approx 1$, base connection lowered to give 7.7 Hz.

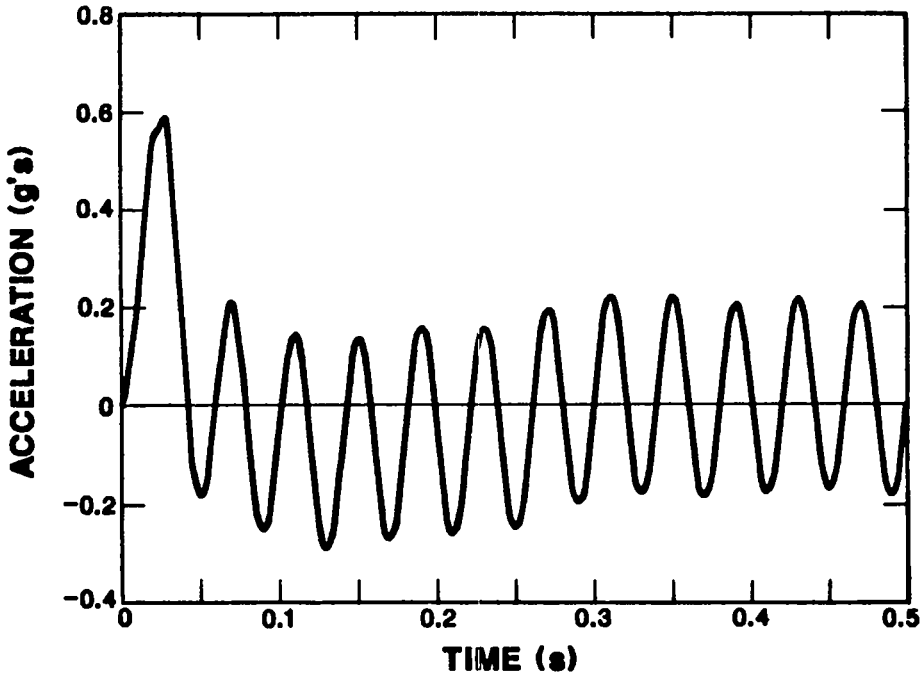

Fig. 24. Time history of node 2 with base connection lowered to give 7.7 Hz and $K_{STRUCTURAL}$ set to theory.

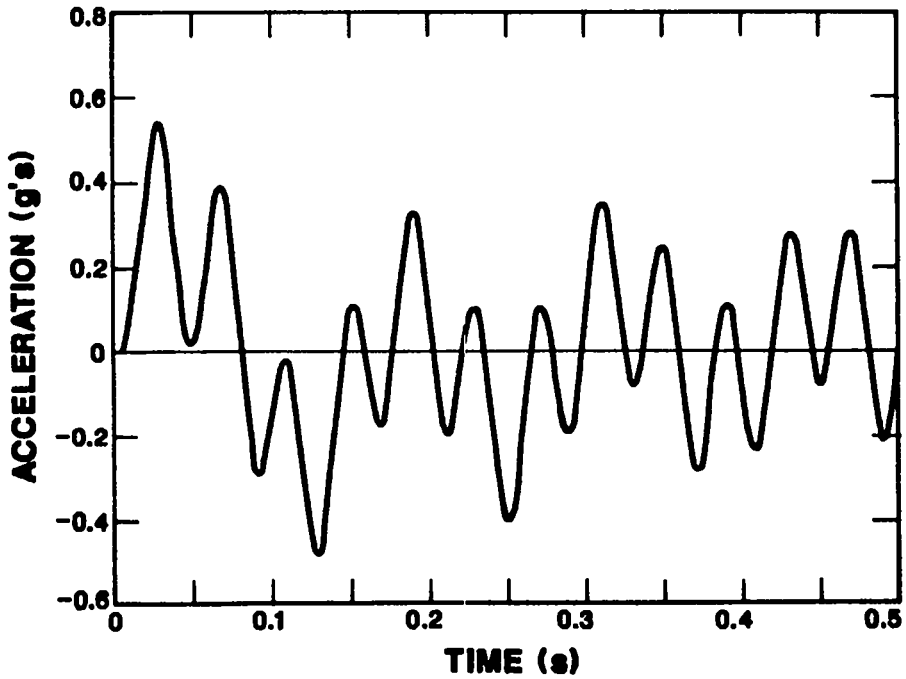

Fig. 25. Time history of node 4 with base connection springs adjusted to give 7.7 Hz and $K_{STRUCTURAL}$ set to theory.

TABLE VII

EFFECTIVE MASSES AND THEORETICAL STIFFNESSES

Test Condition	Effective Mass M.(lb-s^2/in.) TRG-1	TRG-3	Theoretical Stiffness $K_t \times 10^6$ (lb/in.)* TRG-1	TRG-3
A. Free-free, modal test	0.350	22.4	2.90	11.61
B. Fixed-free, no top mass added, modal or base excitation	0.395	25.3	1.27	5.09
C. Fixed-free, top mass added, base excitation	1.917	122.7	See Table V	

* Values computed using "design method" (see Appendix A); $K_{bm} = \infty$.

and B. Values of theoretical stiffness determined for the simulated seismic load conditions (base fixed, mass added) are given in Table V. Values of the theoretical stiffnesses for the free-free modal test condition and the fixed-free, no mass added, modal tests are given in Table VII. All values are computed using $E_c = 57{,}000\sqrt{f'_c} = 3.5 \times 10^6$ psi.

The experimentally determined values of stiffness, for the various test conditions, are shown in Table VIII, together with the theoretically computed values. The ratios of the experimentally determined stiffnesses $\left(K_e\right)$ to the theoretical values $\left(K_t\right)$ are also shown in Table VIII.

The low-load-level static test indicates that

for TRG-1, $K_e = 59\%\ K_t$; and

for TRG-3, $K_e = 86\%\ K_t$.

As previously pointed out, in the discussion of the scalability of two structures, these values seem to indicate that the "real" concrete structure (TRG-3) is relatively stiffer than the microconcrete structures (TRG-1). For reasons previously mentioned i.e., resolution and frame deflection (pp. 14-17), we believe that the value of 86% $\left(\text{for } K_e/K_t, \text{ TRG-3}\right)$ may be too large. In any case, both structures indicate that, even at very low levels of static load

TABLE VIII

COMPARISON OF EXPERIMENTALLY AND THEORETICALLY DETERMINED VALUES OF STIFFNESS

	TRG-1				TRG-3			
Test Condition	Meas Modal Freq, f (Hz)	$K_{experiment}$, K_e $K_e=(2\pi f)^2 M_1$ (lb/in.)*	K_{THEORY}, K_t (lb/in.)	K_e/K_t	Meas Modal Freq, f (Hz)	$K_{experiment}$, K_e $K_e=(2\pi t)^2 M_1$ (lb/in.)*	K_{THEORY}, K_t (lb/in.)	K_e/K_t
A. Static load Test	--	0.75×10^6	1.27×10^6	0.59	--	4.4×10^6	5.09×10^6	0.86
B. Free-Free Modal Test	307.5(#1)	1.30×10^6	2.90×10^6	0.45				
	293.8($3)	1.19×10^6	2.90×10^6	0.41	75.0(#3)	4.97×10^6	11.61×10^6	0.43
C. Fixed-Free No top mass								
1. Modal	221.2(#4)	0.76×10^6	1.27×10^6	0.60	No test			
2. Base excitation	192.6(#5)	0.58×10^6	1.27×10^6	0.46				
3. Base excitation	186.9(#7)	0.54×10^6	1.27×10^6	0.43				
D. Fixed-Free Top mass added								
1. Low-level base motion excitation	76.6(#6)	0.44×10^6	1.25×10^6	0.35	9.5 (0.2 pk#6)	0.45×10^6	5.0×10^6	0.09
					9.0 (0.5 pk#6)	0.39×10^6	(Design Method)	0.08
2. Simulated seismic base excitation	75(#8a)	0.43×10^6	1.25×10^6	0.34	9.4(0.25pk g)	0.43×10^6	5.0×10^6	0.09
	45(#8k)	0.15×10^6		0.12	8.1(2.5pk g)	0.32×10^6		0.06
	75($8a)	0.43×10^6	0.69×10^6 (Structural design method)	0.62	9.4(0.25pk g)	0.43×10^6	2.76×10^6 (Structural design method)	0.16
	75$8a	0.43×10^6	0.68×10^6 (Finite element method-bolts modeled.	0.63	9.4(0.25 g pk)	0.43×10^6	2.71×10^6 (Finite element method-bolts modeled)	0.16

*Except for static test.

(values given are the slope at the origin of the measured load deflection curve), the stiffness is less than the theoretical value computed using a concrete modulus of $57{,}000\sqrt{f'_c}$ (i.e., 3.5×10^6 lb/in. in the structures).

The free-free modal test indicates that

for TRG-1, $K_e = 45\%\ K_t$; and

for TRG-3, $K_e = 43\%\ K_t$.

These data may be the most reliable results from the entire test series since modal frequency can be accurately determined and the assumed free-free boundary conditions may be more nearly satisfied than the fixed-free boundary condition, which is assumed in later tests. Here again, both test structures show that, even at very low-load levels, the stiffness is lower than it would be if computed from theory.

Only the TRG-1 structure was tested with fixed-free boundary conditions and with no added mass on the structure (item C, Table VIII). The value of K_e/K_t of 0.60 (for the modal test) is surprising since it does not fit the trend of constant decrease in stiffness with repeated testing. The other two values (K_e/K_t = 0.46 and 0.43) obtained when the structure is base excited are in good agreement with the results from the free-free modal analysis and would tend to indicate that, with no mass added to TRG-1 on this shake table, the fixed boundary (no base rotation) condition is satisfied.

With the steel plates added to the top of the structure and with the structure clamped to the shake table (item D, Table VIII), the TRG-1 structure appears to suffer further reduction in stiffness, $K_e = 35\%\ K_t$. This value is higher than, but in reasonable agreement with, values (of 25%) reported for the box-like structures tested in FY 1984 (Refs. 3-4). Note that since the acceleration level is the same (± 0.5 g) in tests 5, 6, and 7 (Table IV), the stress level in test 6 is 1.917/0.395 or 4.85* times the stress level in tests 5 and 7.

We believe that this further reduced value of K (K_e = 35% in test 6 as compared to 46 and 43% in tests 5 and 7) is the result of the higher stress level and that this is one of the important characteristics of concrete in

---

* Since stress is proportional to acceleration times mass.

dynamic design and analysis. As was found with other structures tested in FY 1984-85, the TRG-1 structure undergoes progressive reduction in stiffness as the level of the simulated seismic event is increased.

When the steel plates are added to the top of the TRG-3 structure, the structural stiffness appears to undergo a drastic reduction. If this drastic change was caused by additional damage, it was not visible upon inspection at the time of the first seismic test. To pursue the possibility that in this condition there is sufficient base rotation to produce a measured modal frequency considerably lower than the modal frequency associated with shear/loading of the structure, the base connections were theoretically modeled in two ways (Section III) and a theoretical stiffness, which includes the effect of base rotation, was computed (Table V). When the experimentally determined stiffness is compared with these values (K_e = 16% K_t with rotation included), we must conclude that the true structural shear/loading stiffness has been greatly degraded.

VI. CONCLUSIONS

As a result of these findings, it tentatively appears that:

1. If either microconcrete or real concrete structures are carefully constructed and tested, their effective initial low-load-level stiffness can be in the neighborhood of 50% of the value predicted by a mechanics of material calculation using a concrete modulus of $57{,}000\sqrt{f'_c}$.

2. At the low-load level, a microconcrete structure can serve as an adequate model for a real concrete structure.

3. The way in which a real concrete structure's stiffness degrades at higher-load levels cannot be established from this test. However, during these tests, the real concrete structure appears to have suffered <u>more</u> stiffness loss than would be predicted by the microconcrete model.

The authors feel strongly that any further tests to establish the dynamic scalability between "micro" and "real" concrete at higher-load levels should not be conducted using large complete structures because of the inadequacy (in capacity and control) of available test facilities.

VII. REFERENCES

1. E. G. Endebrock, R. G. Dove, and C. A. Anderson, "Margins to Failure - Category I Structures Program: Background and Experimental Plan," Los Alamos National Laboratory report, NUREG/CR-2347 (December 1981).

2. E. G. Endebrock, R. C. Dove, and W. E. Dunwoody, "Analysis and Tests on Small-Scale Shear Walls - FY 82 Final Report," Los Alamos National Laboratory report NUREG/CR-4274 (September 1985).

3. R. C. Dove, E. G. Endebrock, and W. E. Dunwoody, "Seismic Category I Structures Program: Results for Fiscal Years 1983-1984," FY 83-84 report, Los Alamos National Laboratory report, LA-11013-MS, NUREG/CR-4924 (August 1987).

4. E. G. Endebrock, R. C. Dove, and C. A. Anderson, "Seismic Category I Structures Program," Proceedings of the 12th Water Reactor Safety Information Meeting, National Bureau of Standards, Bethesda, Maryland, October 22, 1984.

5. R. C. Dove, E. G. Endebrock, W. E. Dunwoody, and J. G. Bennett, "Seismic Tests on Models of Reinforced Concrete Category I Buildings," presented at the 8th International Conference on Structural Mechanics in Reactor Technology, Brussels, Belgium, August 19-23, 1985, Los Alamos National Laboratory report LA-UR-85-175.

6. J. G. Bennett, R. C. Dove, W. E. Dunwoody, E. G. Endebrock, C. R. Farrar, and P. Goldman, "Simulated Seismic Tests on 1/42- and 1/14-Scale Category I Auxiliary Buildings," Los Alamos National Laboratory report LA-11093-MS, NUREG/CR 4987 (July 1987).

7. J. G. Bennett, R. C. Dove, W. E. Dunwoody, C. R. Farrar, and P. Goldman, "The Seismic Category I Structures Program: Results for FY 1985," Los Alamos National Laboratory report LA-11117-MS, NUREG/CR 4998 (December 1987).

8. W. E. Baker and C. R. Farrar, "Instrumentation for the Upcoming Statistically Planned Experiments on the TRG Structures," note to Technical Review Group, August 1986.

9. D. J. Ewins, Modal Testing (John Wiley & Sons, Research Studies Press Ltd., Letchworth, Hertfordshire, England, June 1985).

10. W. T. Thompson, Vibration Theory and Applications (Prentice-Hall, Englewood Cliffs, NJ, May 1965).

11. R. W. Clough and T. Penzien., Dynamics of Structures (McGraw-Hill, New York, NY, 1975).

APPENDIX A

SAMPLE OF CALCULATIONS INVOLVED IN THE DESIGN METHOD

The assumptions for this method are as follows:

1. assume an uncracked concrete cross section;
2. use the method of transformed sections to transform steel area to concrete and compute the transformed bending area moment of inertia for the cross section, and the transferred effective shear area;
3. use the strength-of-materials approach to compute the stiffness;
4. assume the top and bottom concrete slabs are rigid compared to the cantilever cross section and compute the effective

$$\text{MASS} = M_{ADDED} + M_{SLAB} + M_{DISTRIBUTED}; \text{ and}$$

5. assume that the base is fixed.

The material property values used in these sample calculations are the values used in the original design of the TRG-3 structure, i.e., $E_c = 3 \times 10^6$ psi, $E_{STL} = 30 \times 10^6$ psi. The dimensions and masses are those of the TRG-3 structure.

For the transformed section moment of inertia, consider the shear wall to have N bars on s_1 spaced centers (see Fig. A-1 for definitions of distances). Then, assuming a bar is at the neutral axis, the moment of inertia of the transformed steel is given by

$$I_{STEEL} = N\,\bar{I}_{TRANSFORMED} + \sum i s_1^2\, n\, A_{BAR} \quad , \tag{A-1}$$

where a bar over a quantity is the centroidal value, n is the modular ratio of steel to concrete, A_{BAR} is the cross-sectional area of a reinforcing bar, and i is the multiplier to obtain the distance from the neutral axis.

Now note that the first term in Eq. (1),

$\bar{I}_{TRANSFORMED}$ is approximately $\frac{1}{12}\,ndd^3 = \frac{1}{12}\,nd^4$ where d is the bar diameter.

Generally, this term is neglected since $s_1 > 5d$. For example, for the first bar at s_1, distance from the neutral axis, on 5d centers, the second term in Eq. (1) contributes

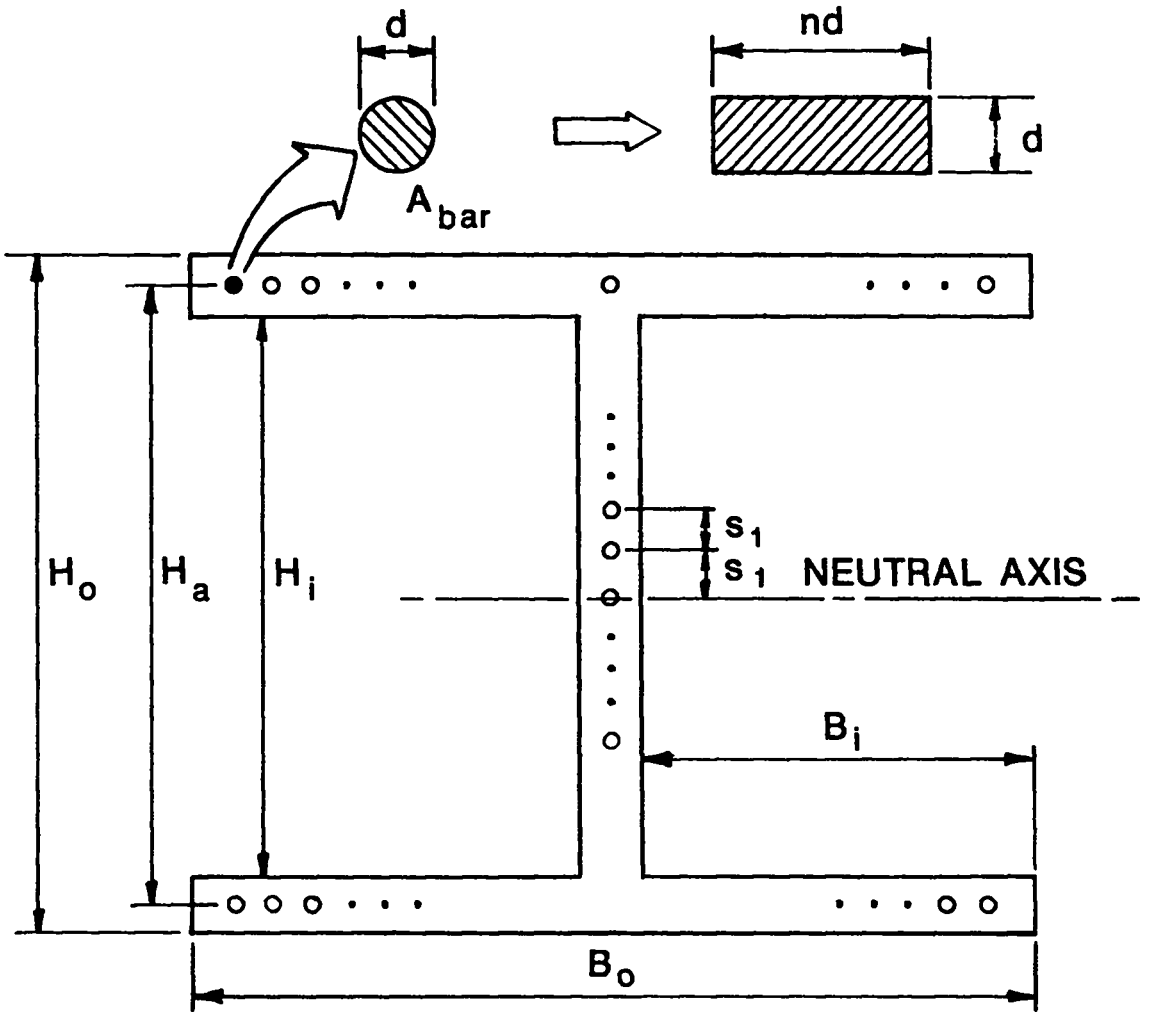

Fig. A-1. Cross section of TRG-3 showing the definition of the distances needed for the transformed section property calculations.

$$s_1^2 \cdot n \cdot A_{BAR} = (5d)^2 n \, A_{BAR}$$

$$= 25d^2 n \frac{\pi d^2}{4} \quad ,$$

$$= \frac{25\pi}{4} nd^4 \quad ,$$

as compared with $\bar{I}_{TRANSFORMED} = \frac{nd^4}{12}$.

The further away from the neutral axis the bar is, the more negligible $\bar{I}_{TRANSFORMED}$ becomes, so that generally Eq. (1) can be written as,

$$I_{STEEL\ TRANSFORMED} = 2 \sum_{i=1}^{N_s} \left(is_1\right)^2 n\, A_{BAR} \quad ,$$

where $N_s = \frac{N-1}{2}$,

where the factor 2 accounts for symmetry of steel above and below the neutral axis. Proceeding in a similar manner, a formula can be developed for the transformed steel in the wing walls.

$$I_{TRANSFORMED\ FLANGE} = 4 \left(\frac{H_A}{2}\right)^2 n\, A_{BAR} N_T \quad ,$$

where

N_T is the number of bars in a wing wall ,
H_A is the distance between wing walls.

If the amount of concrete replaced by the steel is accounted for, the transformed section moment of inertia becomes:

$$I_t = \frac{1}{12}\left[B_0 H_0^{\ 3} - 2B_i H_i^{\ 3}\right] + 2s_1^2\,(n-1)A_{BAR} \sum_{i=1}^{N_s} \left(i^2 + 4(H_A/\ 2)^2 (n-1)A_{BAR} N_T\right) .$$

For the cross section of the TRG-3 structure (Fig. A-1),

B_0 = 120 in.	H_0 = 90 in.	B_i = 58 in.
H_i = 82 in.	s_1 = 4.9 in.	A_{BAR} = 0.11 in.^{2}
N_s = 9	H_a = 86 in.	N_T = 12 ,

and in this example we will take

$$n = \frac{30 \times 10^6 \text{ lb/in.}^2}{3 \times 10^6 \text{ lb/in.}^2} = 10 \quad .$$

If the above numbers are used, the design value for I_t becomes

$$I_t = 2.06 \times 10^6 \text{ in.}^4 \quad .$$

The effective shear area design value is computed as

$$A_e = A_{CONCRETE} + (n - 1)A_{REBAR}N \ ;$$

$$A_e = (90)(4) + (10 - 1)\frac{\pi}{4}\left(\frac{3}{8}\right)^2 19 \quad ;$$

$$A_e = 379 \text{ in.}^2 \quad .$$

The total stiffness (K_T) can now be computed as

$$\frac{1}{K_T} = \frac{1}{K_{CB}} + \frac{1}{K_{SHEAR}} + \frac{1}{K_{BM}} \quad ,$$

in which

K_{CB} is the uncracked cantilever bending stiffness,

K_{SHEAR} is the shear stiffness, and

K_{BM} is the bending moment stiffness due to application of the load through a rigid top plate.

$$K_{CB} = \frac{3E_c I_t}{L^3} = 2.5 \times 10^7 \ \frac{\text{lb}}{\text{in.}} \quad ,$$

$$K_{SHEAR} = \frac{A_e G}{L} = 5.3 \times 10^6 \frac{lb}{in.} ,$$

$$K_{BM} = \frac{2E_c I_t}{hL^2} = 2.5 \times 10^8 \frac{lb}{in.} .$$

Substituting these values into the equation for the total stiffness gives,

$$K_T = 4.3 \times 10^6 \frac{lb}{in.} .$$

To predict the first mode natural frequency we proceed as follows:

$$f = \frac{1}{2\pi}\sqrt{\frac{K_T}{M}} .$$

In this case, the effective mass was calculated as follows:

$$M = M_{ADDED} + M_{SLAB} + M_{DISTRIBUTED}^{*} ,$$

$$M = \frac{37{,}600\ lb}{386\ \frac{in.}{s^2}} + \frac{7{,}500\ lb}{386\ \frac{in.}{s^2}} + \frac{33}{140}\ \frac{144\ \frac{lb}{ft^3}}{1728\ \frac{in.^3}{ft^3}}\ \frac{1}{386\ \frac{in.}{s^2}}\ 1288\ in.^2\ (90\ in.) ,$$

$$M = 97.4 + 19.4 + 5.9 = 122.7\ \frac{lb\text{-}s^2}{in.} .$$

Then

$$f_{PREDICTED} = \frac{1}{2\pi}\sqrt{\frac{4.3 \times 10^6 \frac{lb}{in.}}{122.7\ \frac{lb\text{-}s^2}{in.}}} , \qquad f_{PREDICTED} = 29.8\ Hz.$$

---

* The factor (33/140) is from the "Rayleigh Method" analysis. See example 1.5-3, p. 19 of Ref. 10.

APPENDIX B

A STRUCTURAL DYNAMICS METHOD OF ANALYZING TRG-3

The details of this approach are summarized here. The notation is as follows:

M	=	generalized mass
K	=	generalized stiffness
$\psi(y)$	=	the shape function of the coordinate y
B	=	subscript indicating bending
S	=	subscript indicating shear
R	=	subscript indicating rigid body rotational effect
a	=	bending deformation proportional constant
b	=	shear deformation proportional constant
c	=	rotational deformation proportional constant
$\sum$	=	$a + b + c$
L	=	length
$\psi'(y)$	=	derivative of ψ with respect to y
$U_g(t)$	=	ground displacement as a function of time
$\dot{U}_g(t)$	=	a dotted quantity indicates time derivative, in this case ground velocity
T	=	kinetic energy of the system
V	=	potential energy of the system
p_{eff}	=	generalized effective forcing function
K_t	=	torsional spring constant for base slab connections
m	=	mass per unit length
J_0	=	rotation movement of inertia about base rotational axis
M	=	rigid mass (top slab + added weights)

GENERALIZED COORDINATES (Fig. B-1).

Kinematic relations:

$$v^*(y,t) = U_g(t) + v(y,t) \quad .$$

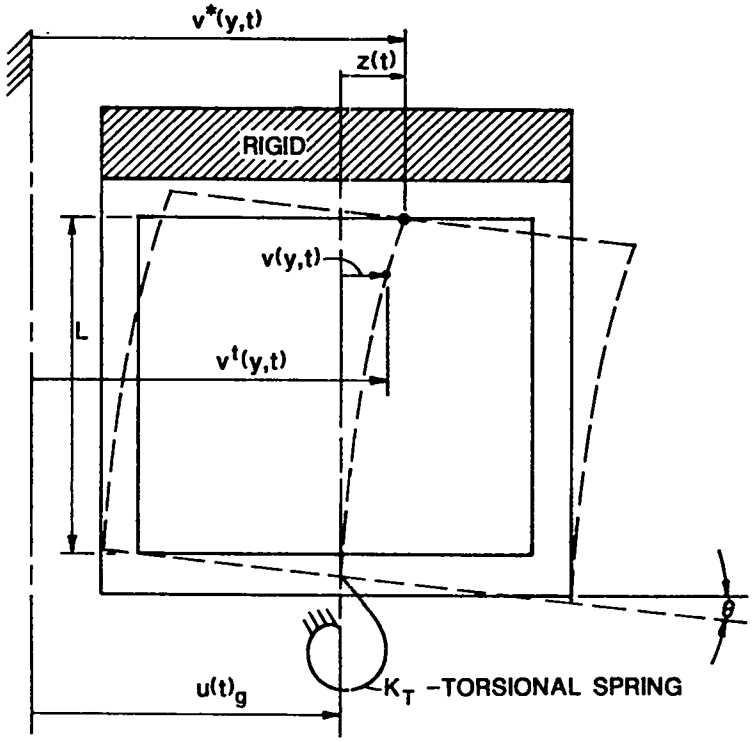

Fig. B-1. Definitions of the coordinates used in this analysis.

Assumptions:

$$v(y,t) = \psi(y)Z(t);$$

$$v^*(y,t) = U_g(t) + \psi(y)Z(t), \text{ and}$$

$$\dot{v}^*(y,t) = \dot{U}_g + \psi(y)\dot{Z}(t) \quad ,$$

where ψ is the shape function.

Kinetic energy of the system:

$$T = \int_0^L \frac{1}{2} m(y)\left[\dot{v}^*(y,t)\right]^2 dy + \frac{1}{2} J_0 \dot{\theta}^2 + \frac{1}{2} M\left[\dot{v}^*(L,t)\right]^2 .$$

Potential energy of the system:

$$V = \int_0^L \frac{1}{2} E_c I_t \left[v_B''\right]^2 dy + \int_0^L \frac{1}{2} GA_e \left[v_s'\right]^2 dy + \frac{1}{2} K_t \theta^2 .$$

Shape function requirements:

$$\psi(y) = \begin{cases} 1 \ @ \ y = L \\ 0 \ @ \ y = 0 \end{cases} .$$

Shape function choice (based on Fig. B-2):

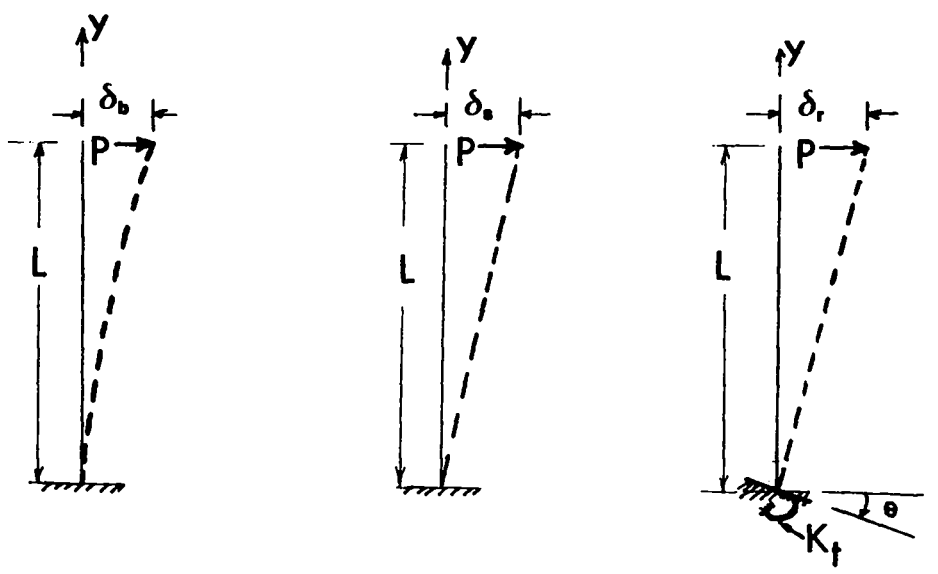

$$\delta_b = \frac{PY^3}{3EI}\Bigg|_{y=L} \qquad \delta_s = \frac{PY}{A_s G}\Bigg|_{y=L} \qquad \delta_r = \frac{PLY}{K_t}\Bigg|_{y=L}$$

Fig. B-2. The combination of shapes used to define the shape function in the analysis.

$\psi = \psi_B + \psi_S + \psi_R = \frac{1}{\Sigma} a\left(\frac{y^3}{L^3} + b\,\frac{y}{L} + c\,\frac{y}{L}\right)$. The letters a, b, and c are proportionality constants.

Clearly,

$$\frac{a}{b} = \frac{\delta_B}{\delta_S} = \frac{K_S}{K_B} \quad ,$$

$$\frac{b}{c} = \frac{\delta_S}{\delta_R} = \frac{K_R}{K_S} \quad .$$

If we choose a = 1 and substitute the appropriate values for K_S, K_b, b and c can be determined.

Hamilton's principle:

$$\int_{t_1}^{t_2} \delta\,(T - V)dt = 0 \quad ,$$ leads to the following results.

Generalized equation of motion:

$$M\ddot{Z} + KZ = -p_{eff} \quad .$$

Generalized mass:

$$M = \int_0^L m\left[\psi(y)\right]^2 dy + J_0\left(\psi_R'\right)^2 + M \quad .$$

Generalized stiffness:

$$K = \int_0^L E_I\left[\psi_B''(y)\right]^2 dy + \int_0^L GA_e\left[\psi_S'(y)\right]^2 dy + k_t\left[\psi_R'(o)\right] \quad .$$

Generalized forcing function:

$$p_{eff} = \ddot{U}_g(t) \int_0^L m\,\psi(y)dy + M\ddot{U}_g \quad .$$

These equations are subject to quiescent initial and final conditions:

$$\dot{U}_g(o) = \dot{Z}(o) = \dot{U}_g(f) = \dot{Z}(f) = 0 \quad .$$

First mode frequency:

$$f = \frac{1}{2\pi}\sqrt{\frac{K}{M}} \quad .$$

Carrying out details will lead to the following expressions for K and M:

$$K = \frac{9a^2}{\Sigma^2}\frac{E_c I_t}{L^3} + \frac{b^2}{\Sigma^2}\frac{GA_e}{L} + \frac{c^2}{\Sigma^2}\frac{K_t}{L^2} \quad ,$$

$$M = \frac{mL}{105\,\Sigma^2}\left[15a^2 + 42a(b + c) + 35(b + c)^2\right] + J_0\frac{c^2}{\Sigma^2 L^2} + M_{ADDED} \quad .$$

Evaluation of $K_{torsional}$:

If the TRG-3 structure slab is assumed to be precompressed onto the table by the bolt connection system, the torsional spring constant can be approximated. The further assumptions are that no gaps open between the model and

the table during the test and that the effective concrete compressional zone under each bolt/plate connection can be approximated as an axial spring. For the TRG-3 connection, it is estimated that the product of the compressional area, A and E_c are approximately the same as the AE product of bolts. Thus, doubling the effective length of each bolt approximately accounts for concrete compression. Further, assuming that the TRG-3 structure "rocks" as a rigid body about its neutral axis allows the torsional spring to be calculated as

$$K_t = \sum_{i=1}^{\substack{\text{all}\\ \text{bolts}}} R_i^2 \frac{AE}{L_{eff}} ,$$

where R_i is the perpendicular distance from the rocking axis to the ith bolt. Using the bolt pattern shown in Fig. A-3, and $E = 30 \times 10^6$ lb/in.^{2}, $A = 0.969$ in.^{2}, and $L_{eff} = 16$ in., K_t can be evaluated as

$$K_t = 3.58 \times 10^{10} \frac{\text{in.} - \text{lb}}{\text{radian}} .$$

This value was used to calculate the results in Table B-1.

Using the parallel axis theorem and breaking the structure into parts, the rotational mass moment of inertia about the base axis of rotation can be approximated as

$$J_0 = \sum_{\text{all}}^{\text{parts}} (\bar{J} + d^2M) = 2.03 \times 10^6 \text{ in.-lb-s}^2 ,$$

where $\bar{J}$ is the mass moment of inertia about an axis parallel to the base passing through the mass center of the part, d is the distance from the axis to the base axis, and M is the mass of the part.

This value of J_0 is used for the results shown in Table B-1.

TABLE B-1

CONSTANTS USED AND RESULTS

E_c $\left(\frac{lb}{in.^2}\right)$	a -	b -	c -	L (in.)	I_t $\left(in.^4\right)$	K (lb/in.)	M $\left(\frac{lb\text{-}s^2}{in.}\right)$	f_n (Hz)
3.5×10^6	1	4.72	6.5	90	2.06×10^6	2.76×10^6	195.5	18.9
3.0×10^6	1	4.72	5.61	90	2.06×10^6	2.59×10^6	186.0	18.8
2.0×10^6	1	5.0	4.09	90	2.15×10^6	2.11×10^6	165.6	18.0

DISTRIBUTION

	Copies
Nuclear Regulatory Commission, RW, Laurel, Maryland	248
Technical Information Center, Oak Ridge, Tennessee	2
Los Alamos National Laboratory, Los Alamos, New Mexico	50
	300

NRC FORM 335 (12-84) NRCM 1102, 3201, 3202

U.S. NUCLEAR REGULATORY COMMISSION

BIBLIOGRAPHIC DATA SHEET

SEE INSTRUCTIONS ON THE REVERSE

1 REPORT NUMBER (Assigned by TIDC, add Vol. No., if any)

NUREG/CR-5182
LA-11377-MS

2 TITLE AND SUBTITLE

The Seismic Category I Structures Program: Results for FY 1986

3 LEAVE BLANK

4 DATE REPORT COMPLETED

MONTH	YEAR
June	1988

5 AUTHOR(S)

J.G. Bennett, R.C. Dove, W.E. Dunwoody, C.R. Farrar, P. Goldman

6 DATE REPORT ISSUED

MONTH	YEAR
September	1988

7 PERFORMING ORGANIZATION NAME AND MAILING ADDRESS (Include Zip Code)

Los Alamos National Laboratory
Los Alamos, NM 87545

8 PROJECT/TASK/WORK UNIT NUMBER

9 FIN OR GRANT NUMBER

A7221

10 SPONSORING ORGANIZATION NAME AND MAILING ADDRESS (Include Zip Code)

Division of Engineering
Office of Nuclear Regulatory Research
U.S. Nuclear Regulatory Commission
Washington, DC 20555

11a TYPE OF REPORT

Technical

b PERIOD COVERED (Inclusive dates)

12 SUPPLEMENTARY NOTES

13 ABSTRACT (200 words or less)

The accomplishments of the Seismic Category I Structures Program for FY 1986 are reported. The background leading to the FY 1986 Program Plan is summarized and the design of a new geometric configuration of a reinforced concrete shear wall test structure is described. The report discusses static and seismic testings of two of these structures, a 1/4-scale, 1-in.-thick shear wall model of microconcrete and a 4-in.-thick shear wall prototype. Results and conclusions regarding degrading stiffness characteristics, natural frequencies, and scalability of microconcrete with actual concrete are compared with past fiscal year results. Possible base rotation effects for the large structure are examined analytically. Finally, tentative conclusions are stated regarding the degrading stiffness and scaling of these structures and recommendations are made about future seismic testing of large structures.

14 DOCUMENT ANALYSIS a. KEYWORDS/DESCRIPTORS

Reinforced Concrete Shear Wall Structures, Modal Testing, Static Testing, Simulated Seismic Testing

b. IDENTIFIERS/OPEN ENDED TERMS

15 AVAILABILITY STATEMENT

Unlimited

16 SECURITY CLASSIFICATION

(This page)
Unclassified

(This report)
Unclassified

17 NUMBER OF PAGES

18 PRICE

UNITED STATES
NUCLEAR REGULATORY COMMISSION
WASHINGTON, D.C. 20555

OFFICIAL BUSINESS
PENALTY FOR PRIVATE USE, $300

SPECIAL FOURTH-CLASS RATE
POSTAGE & FEES PAID
USNRC

PERMIT No. G-67

NOV 14 1988
RECEIVED